INTERFACIAL ELECTRON TRANSFER IN COLLOIDAL METAL AND SEMICONDUCTOR DISPERSIONS AND PHOTODECOMPOSITION OF WATER

KUPPUSWAMY KALYANASUNDARAM and MICHAEL GRÄTZEL

Institut de Chimie Physique, Ecole Polytechnique Fédérale, CH-1015 Lausanne (Switzerland)

EZIO PELIZZETTI

Dipartimento di Chimica Analitica Università di Torino I-10125 Torino (Italy)

CONTENTS

A. INTRODUCTION

The global energy crisis of the seventies has had a very pronounced influence on the scientific community. It has forced them to make a hard

assessment of the future world energy supply, realize the fast-dwindling situation of the fossil fuel reserves and seek to develop alternative energy sources. Fossil energy resources are provided by natural photosynthesis, a fascinating process which has been widely investigated. Light-induced charge separation is achieved through judicious spatial arrangement of the pigments and the elements of the electron transport chain in the thylakoid membrane. Cooperative interactions between these components allows the electron transfer to proceed in a vectorial fashion. Enzymes play the role of catalysts which couple the charge separation events to fuel-generating reactions. A major goal of all "studies in vitro" has been to simulate this photosynthetic quantum machinery and adopt it to cleave water into H_2 and O_2 using visible light. While artificial photoconversion devices should not attempt to imitate all the intricacies of natural photosynthesis, it is inconceivable that the challenging task of driving endergonic chemical reactions such as cleavage of water can be achieved without suitable engineering at the molecular level.

Admittedly, photochemical conversion of solar energy is a very broad area with several potential approaches possibly leading to practical devices in the not too distant future. In this review, we will survey some of these areas, areas of personal interest and experience. Fortunately the field of photochemical conversion and storage of solar energy is blessed with numerous periodical reviews, including some from our own laboratories [1–16]. Hence, our approach in this review is somewhat restrictive in that, in addition to broadly outlining the progress and the status in a few areas, we selectively review recent studies. Thus, in many aspects, this is a complementary and up-dated version of an earlier survey in 1980 [8].

Catalytic schemes for the photodecomposition of water and other photoredox reactions of interest consist essentially of two steps: (a) light-induced generation of strong oxidants and reductants capable of oxidizing/reducing water

$$S + A \underset{}{\overset{h\nu}{\rightleftarrows}} S^+ + A^- \tag{1}$$

(b) redox catalytic decomposition of water using the photogenerated species and suitable catalyst materials

$$4S^+ + 2H_2O \overset{cat_1}{\rightarrow} 4S + 4H^+ + O_2 \tag{2}$$

$$2A^- + 2H_2O \overset{cat_2}{\rightarrow} 2A + 2OH^- + H_2 \tag{3}$$

Photoredox cycles involving homogeneous dyes (e.g. transition metal polypyridine complexes, metalloporphyrins and organic dyes such as acridines) are the simplest systems to explore. One of the major problems in the

effective utilization of these dyes in homogeneous solutions is that the energy saving (uphill) electron transfer reactions such as those depicted in reaction (1) are accompanied by very efficient (diffusion-controlled) reverse electron transfer steps regenerating the starting materials. This restricts the lifetimes of photogenerated species to a few microseconds. For practical utility one needs very efficient as well as selective redox catalysts to prevent the reverse electron transfer via reactions such as (2) and (3). Development of these extremely efficient catalysts has indeed been very difficult.

There are several approaches that can be envisaged to overcome the above difficulties. One simple way is to prevent the reverse electron transfer chemically with another (a third component) oxidant or reductant to reduce or oxidize rapidly one of the electron transfer products of reaction (1). Here again, those donors/acceptors which undergo rapid decomposition

$$S^+ + D \rightarrow S + D^+ \tag{4}$$

or disproportionation upon oxidation/reduction are those which are most effective for the obvious reason, i.e. continued presence of oxidizing or reducing radicals derived from either reactions (1) or (4), can only facilitate undesirable reverse electron transfers. In recent years, several such modified photoredox schemes (known as "sacrificial systems" to emphasize the irreversible decomposition of the third component) have been identified and subjected to very intensive study. Redox catalysts, both homogeneous and heterogeneous, are now known and with these it is presently possible to photodissociate water into either hydrogen or oxygen with reasonable quantum efficiencies. A broad overview of such systems using heterogeneous and homogeneous catalysts for light-induced generation of H_2 and O_2 (from water is presented in Sections C and D respectively.

It should be emphasized, that in photochemical systems that generate one-electron oxidants and reductants, introduction of redox catalysts to promote multi-electron transfer has been primarily responsible for the recent success in photodecomposition of water into molecular oxygen or hydrogen. Consequently, a fairly large amount of research effect has gone into the identification, preparation, characterization and assay of redox catalysts, and also into the mechanistic details on their mode of operation in reactions such as (2) and (3). Section E provides a broad summary of these studies.

Another approach for attacking the problem of reverse electron transfer, which has now been intensively pursued for over a decade, is the use of organized molecular assemblies to achieve the light-induced charge separation step. The idea is to separate spatially the reactants and products on a microscopic scale using the inherent differences in their hydrophobicity or hydrophilicity, and through the introduction of charged interfaces. Alternatively, one or other reactant can be functionalized on a particular site in a

macromolecular host system by appropriate molecular design or through chemical derivatization.

Yet another fairly recent approach, is to use semiconductor-particulate systems and colloids as light absorbing units. The advantage with semiconductors is that light-induced oxidation–reduction reactions are very often irreversible. As with homogeneous dye-based systems, the semiconductor dispersions can be loaded with suitable redox catalysts to facilitate the generation of multi-electron transfer oxidation–reduction products. This is often a necessity, for most of the known semiconduction materials are inherently poor catalyst materials for the overall chemical reactions of interest. Section F is concerned with the progress in the photodissociation of water using semiconductor dispersions. In addition to photodecomposition of water, photogeneration there is a large number of other photoredox reactions that have been, and are being studied, in semiconductor particulate systems, and a broad survey of this topic can be found in refs. 15 and 16. We briefly address some key areas.

For the reasons just mentioned with semiconductor particulate systems, i.e. the lack of catalytic activity by the semiconductors themselves, introduction of redox catalysts on the surface of a semiconductor electrode is beneficial. There is an increasing number of photoelectrochemical cell studies with semiconductor electrodes that utilize catalyst films or coatings to generate useful chemical products. With p-type semiconductors such as p-InP coated with Pt-group metals, it is now possible to photogenerate H_2 from water with over 10% solar-to-chemical conversion efficiency. Section F also includes a brief discussion of these studies.

Colloidal semiconductors offer a number of very desirable properties such as high extinction coefficients, fast carrier diffusion to the interface and suitable positioning of valence and conduction bands to achieve high efficiencies in light-energy conversion processes. The transparent nature of these sols allows a ready detection of short-lived intermediates by fast kinetic spectroscopy. Thus, it is now possible to monitor directly the kinetics of heterogeneous electron-transfer reactions of electrons and holes with oxidants–reductants present in the solution. With finely-dispersed colloidal semiconductor sols, it is also possible to monitor photoluminescence readily, and this greatly enhances our ability to monitor photoprocesses following bandgap excitation. Section G outlines some of these methods and also describes recent progress in this exciting field.

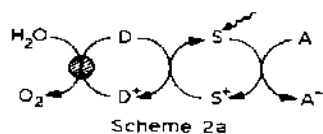## B. PHOTOREDOX SCHEMES FOR THE LIGHT-INDUCED OXIDATION AND REDUCTION OF WATER

Before we embark on a review of various components and catalyst material that go to constitute various water photolysis systems, it is pertinent

(oxidative cycle)
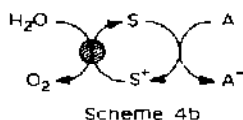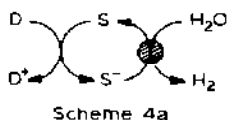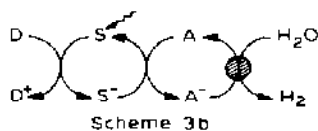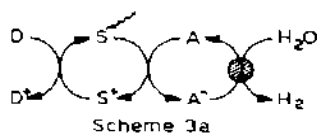Scheme 1a

(reductive cycle)
Scheme 1b
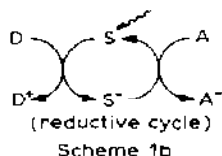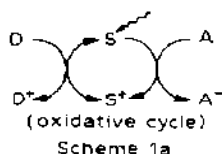
to outline briefly the various photoredox schemes which can generate suitable strong oxidants and reductants capable of oxidizing or reducing water. In systems for the light-induced evolution of H_2 from water, photogeneration of a reduced acceptor relay is required, and this is readily achieved in a three-component ("sacrificial") system consisting of a photosensitizer S, an electron acceptor A and an electron donor D. The various reactions that follow light excitation of the sensitizer are succinctly summarized in Schemes 1a and 1b. Scheme 1a constitutes an "oxidative redox cycle" in which the excited sensitizer S^* is quenched by the acceptor relay A (to give S^+ and A^-) and the oxidized sensitizer is subsequently reduced to its initial ground state by the third component, the electron donor D. Alternatively, the same overall products (D^+, A^- and S) can also be derived via a "reductive redox cycle" as shown in Scheme 1b. Here, the added electron donor D acts as the quencher of S^* and the reduced sensitizer S^- is subsequently oxidized by the acceptor relay A. The occurrence of an oxidative or reductive cycle in a given system depends on the excited state redox potentials of S^* [$E(S^+/S^*)$, $E(S^*/S^-)$], the redox potentials of the donor, the acceptor relays and their actual concentrations in the photolysis solution.

With mild donors and sensitizers which are strong reductants in the excited state, an oxidative cycle invariably operates. For solar or visible light excitation, the overall efficiency for the generation of D^+ and A^- depends on the light adsorption properties of the sensitizer, the efficiency of photoredox quenching, the cage escape yields, and last but not least, the extent and severity of fast thermal reverse electron transfer reactions.

In the presence of suitable redox catalyst materials, catalytic reaction steps such as reactions (2) and (3) are coupled to Schemes 1a and 1b to give molecular oxygen (Scheme 2) or molecular hydrogen (Scheme 3). For reactions such as (2) and (3) to occur in the dark with reasonable efficiency, thermodynamic energy requirements demand [$E(A/A^-) < E(H^+/H_2)$] and [$E(D^+/D) > E(O_2/H_2O)$]. In systems such as those shown in Schemes 2 and 3, with appropriate sensitizer materials, it is possible to couple the
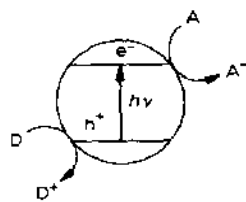

Scheme 2a

Scheme 2b

D S A H$_2$O
D$^+$ S$^-$ A$^-$ H$_2$
Scheme 3a

D S A H$_2$O
D$^+$ S$^-$ A$^-$ H$_2$
Scheme 3b

D S H$_2$O
D$^+$ S$^-$ H$_2$
Scheme 4a

H$_2$O S A
O$_2$ S$^+$ A$^-$
Scheme 4b

primary photoredox reaction to the redox catalytic steps directly (Schemes 4a and 4b). These are simpler two-component systems which can generate H$_2$ or O$_2$ from water. One of the major problems in systems such as that shown in Scheme 4a is that very often protonation of the reduced dyes occur very rapidly, followed by rapid disproportionation (e.g. with acridine dyes and metalloporphyrins) in competition with redox catalytic steps (eqns. 5 and 6)

$$S^- + H^+ \rightarrow SH^{\cdot} \tag{5}$$

$$2SH^{\cdot} \rightarrow S + SH_2 \tag{6}$$

Similarly, with systems such as that shown in Scheme 4b, strong oxidants such as S^+ oxidize other species present in the solution or undergo simple decomposition. For this reason, it is advantageous to regenerate the sensitizer S from S^- and S^+ rapidly. Fortunately, a few electron donor materials are known which can also play the role of the redox catalyst and promote water oxidation to molecular oxygen upon photooxidation, as well as a few acceptor relays which can spontaneously catalyze water reduction to molecular hydrogen. With these examples, homogeneous catalysis is coupled to photoredox reactions. The performance of various sensitizers, electron acceptors and donors and catalyst materials in the above water photolysis schemes are reviewed in the subsequent sections, first with systems which utilize externally-added heterogeneous catalysts (including colloidal redox catalysts) (Section C) and second with systems which involve homogeneous catalysis as an integral part of the photolysis cycle (Section D).

With semiconductor systems, bandgap excitation leads to generation of electron-hole pairs, and under the influence of the space charge layer separation of these occurs. In dispersion systems, these species, upon migration to the surface, are available for redox reactions (Scheme 5). On n-type semiconductor electrodes, the photogenerated holes move over to the surface causing oxidations at the illuminated semiconductor electrodes. The electrons flow in the opposite direction to the back contact and finally arrive at the counter electrode for reduction reactions (Scheme 6a). An inverse situation occurs with p-type semiconductor electrodes (Scheme 6b).

Scheme 5

Photooxidation at SC electrode

Photoreduction at SC electrode
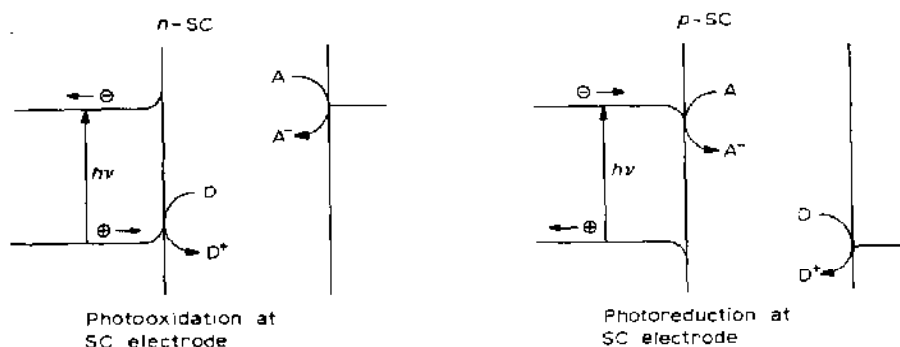
Scheme 6

To a first approximation, under illumination (saturation level), electrons and holes are delivered at potentials corresponding to E_{cb} and E_{vb}, though the free energy (quasi-Fermi) levels of these are readily perturbed by the nature of the solvent, the presence of ions adsorbing or reacting with the semiconductor surface, and the presence of surface states and surface charges. Here again, the overall efficiency of the system depends on the magnitude of the bandgap, the location of band edges, the efficiency of charge carrier generation (depending on several factors such as mobility, etc.), the role of the semiconductor–electrolyte interface, the kinetic barriers for electron transfer reactions of interest at the interface, and on the prevention of photocorrosion. For the reasons discussed, to achieve photolysis of water into molecular H_2 and O_2, it is necessary, except probably with large bandgap oxide semiconductors, to coat the semiconductor (electrodes and dispersions) with suitable catalyst materials.

C. PHOTODECOMPOSITION OF WATER IN HOMOGENEOUS DYE-BASED SYSTEMS USING HETEROGENEOUS REDOX CATALYSTS

(i) Photoproduction of H_2 from water

Studies of the photochemical conversion of solar energy have received a significant boost in the last six to seven years with the discovery of several

TABLE 1

Candidates for three-component dye-based systems for light-induced H_2 evolution from water

Sensitizers	Acceptors	Catalysts	Donors
Polypyridine Complexes of Transition Metals $M L_n^{m+}$, L = bpy, bpz, phen,.. M = Ru, Cr, Rh,..	*Quaternary bipyridinium and phenanthrolinium salts* MV^{2+}, PVS,...	*Enzymes* H_2-ases and N_2-ases	*EDTA and other aminoacids*
		Metal oxides: PtO_2, RuO_2, IrO_2,...	*S compounds* Cysteine, H_2S, mercaptoethanol,...
Metalloporphyrins Tetramethylpyridylporphyrins (TMPyP^{4+}) of Zn, Sn(IV), Pd,...	*Stable Metal Ions and Metal Complexes*	*Colloidal Metals:*	*Amines*
Tetrasulfonatophenylporphyrins (TPPS^{4-}) of Zn, Cd, Mn	Salicylate, EDTA complexes of V, Cr and Eu(III)	Pt, Cd, Ag, Au, Ir	TEA, TEOA, ascorbate
	Co cage-complexes Co(sepul)$^{3+}$, Co(diarsen)$^{3+}$		*Simple Metal Ions* Eu(II), Fe(II),...
Tetraaminophenylporphyrins (TAPP^{4+}) of H_2, Zn,...	*Labile Complexes of Co, Rh,..* CoL_n^{m+}, L = bpy, dmgH,..., Rh(bpy)$_3^{3+}$, Rh(bpy)$_2$Cl$_2$,..		
Tetraphenylporphyrins (TPP) of Zn, Rh, Mg,.. Uro, copro, protoporphyrins of Zn, Sn(IV),..			
Phthalocyanines Mg, ZnPc, ZnPcS^{4-}			
Heteropolyacids of Mo, W, V			
Other metal complexes Metal–sulfur chelates, Pt–NEt$_n$ complexes,...			
Organic dyes			
Acridines: proflavine, acridine orange, acridine yellow			
Fluoresceins: dibromofluorescein			
Cyanines: neocyanine, pinacyano carbocyanines, anthracene carboxylates			

photosystems that efficiently evolve molecular H_2 from water upon visible light excitation. Table 1 provides a summary of various components so far identified as candidates for utilization as S, D, A and as catalysts for the three-component photoredox systems just elaborated. A conference volume edited by Harriman and West [4] bears witness to the numerous studies on "sacrificial" systems that have been reported in the last few years. Though the types of compounds explored and found to be effective are numerous, the number of photosystems that have been subject to detailed mechanistic study have been few. Fortunately, the information available to date is quite adequate to define broadly the scope, potentialities and limitations of these systems for the light-induced evolution of H_2 from water.

In photosystems based on systems set out in Schemes 3a, 3b and 4a, there are two factors which define the overall efficiency of the photosystem in liberating H_2: firstly, the cage escape yields in the primary photoredox quenching step (ϕ_{cage})

$$S + A \underset{}{\overset{h\nu}{\rightleftarrows}} S^+ + A^- \left(\phi_{cage} \right) \tag{7}$$

$$S + D \underset{}{\overset{h\nu}{\rightleftarrows}} S^- + D^+ \left(\phi_{cage} \right) \tag{8}$$

i.e., the yield of free, solvated ions that escaped recombination in the primary cage and are available to take part in subsequent redox catalytic steps. Secondly, the efficiency (η_{cat}) of the redox catalysis step itself

$$2A^- + 2H_2O \overset{cat_1}{\rightarrow} 2A + 2OH^- + H_2 \tag{9}$$

$$4D^+ + 2H_2O \overset{cat_2}{\rightarrow} 4D + 4H^+ + O_2 \tag{10}$$

Under optimal conditions, the overall quantum yield for hydrogen generation (ϕ_{H_2}) is given by the product of these two efficiencies

$$\left(\phi_{0.5\,H_2} \right) = \left(\phi_{cage} \right) \left(\eta_{cat} \right) \tag{11}$$

Table 2 summarizes available data on ϕ_{cage} and on ϕ_{H_2} for various photosystems [17–53].

A priori, the individual efficiencies of the two key steps are expected to approach unity. Several finely divided, active colloidal redox catalysts are now known with which $\eta_{cat} \sim 1.0$, but ϕ_{cage} values span a wide range from 0.001 to 1.0. Mechanisms and efficiencies of photoredox reactions in general have been the subject of detailed analysis in recent years, especially in the groups of Sutin, Meyer, Endicott, Balzani and Scandola, and much greater appreciation of the factors influencing the cage escape yields has been obtained [54,55,56–61]. Hence, a more intelligent approach to the design of

TABLE 2

Quantum efficiencies for photogeneration of reduced relays and for hydrogen evolution from water

Sensitizer	Acceptor	Donor	Mechanism	ϕ_{cage}	Catalyst	ϕ_{H_2}	Ref.
Dibromofluorescein	–	TEOA	Red.		Pt/TiO₂	0.1 (pH 12.5)	17
Alkylammonium isopolyvanadate	–	H₂O?	Red.		–	0.002 (pH 9.5)	18
9-Anthracene-COO⁻	MV²⁺	EDTA	Ox.	0.91 (385 nm)	Pt-PVA	0.465 (pH 5.0)	19
9-Anthracene-COO⁻ + Ru(bpy)₃²⁺	MV²⁺	EDTA	Ox.		Pt-PVA	0.425 (pH 5.0)	20
Ru(bpy)₃²⁺	MV²⁺	EDTA	Ox.	0.25	Pt-PVA	0.045	20
Alkylammonium-polytungstate	–	H₂O?	Red.		–	0.05 (pH 7.0)	21
Ru(bpy)₃²⁺	Co(dmgH)₂	TEOA/DMF	Red.		–	0.13	22
Ru(bpy)₃²⁺	Co(sepul)³⁺	EDTA	Ox.	0.05?	Pt-PVA	0.04 (pH 5)	23
Ru(bpy)₃²⁺	Co(azacapten)²⁺	EDTA	Ox.	0.6		–	23
NaVO₃, VOCl₃	–	Alcohols	Red.	0.068 (iPrOH)		0.033 (iPrHOH)	24
				0.026 (EtOH)		0.012 (EtOH)	24
				0.08 (MeOH)		0.111 (MeOH)	24
				0.05 (iBuOH)			24
Ru(bpy)₃²⁺	MV²⁺	EDTA	Ox.	0.8?	Pt	0.07	24
Proflavine	MV²⁺	EDTA	Red.	0.9?	Pt	0.18	25
Acridine yellow	MV²⁺	EDTA	Red.	0.9?	Pt	0.15	25
Ru(bpy)₃²⁺	MV²⁺ and other viologens	EDTA	Ox.	0.13?			26
Dodecawol-framasilicic acid	–	CH₃OH	Red.		Pt	0.1 (340 nm)	27
Ru(bpy)₃²⁺	Co(sepul)³⁺	EDTA	Ox.	0.9?	Pt-Carbowax		28
Ru(bpy)₃²⁺	Co(Me₂-bpy)₃³⁺	Asc.	Red.	0.5	–	0.13 (pH 5)	29
Ru(bpy)₃²⁺	Polymeric viologen	EDTA	Ox.	0.12	Pt-PVA	0.05	30
Ru(bpy)₃²⁺	MV²⁺	EDTA	Ox.	0.10?	Pt-PVA		31
	TMV²⁺			0.08			31
	HMV²⁺			0.05			31

Sensitizer	Relay	Donor	Ox./Red.	Φ	Catalyst	Φ	Ref.
Zn-Chl a	MV^{2+}	EDTA/DMSO	Ox.	0.40			32
Mg-Chl a	MV^{2+}	EDTA/DMSO	Ox.	0.23			32
Cu-Chl a	MV^{2+}	EDTA/DMSO	Ox.	0.13			32
$Ru(bpy)_3^{2+}$	MV^{2+}	–	Ox.	0.25			32
$Ru(bpy)_3^{2+}$	$Os(NH_3)_5Cl^{2+}$	Asc.	Red.	0.5	–	$\leq 10^{-3}$	33
		Eu^{2+}	Red.				33
$Ru(bpy)_3^{2+}$	Ti^{2+}	–	Ox.		–	$< 10^{-5}$	34
$Ru(bpy)_3^{2+}$	MV^{2+}	EDTA	Ox.	0.22	Pt-PVA	0.059–0.096	35
$Ru(bpy)_3^{2+}$	MV^{2+}	EDTA	Ox.	0.30	Pt-PVA	0.13	36
$ZnTMPyP^{4+}$	MV^{2+}	EDTA	Ox.	0.75	Pt-PVA	0.30	37
$ZnTMPyP^{4+}$	–	EDTA	Red.	0.08	Pt-PVA	0.015	38
$ZnTMPyP^{4+}$	–	EDTA	Red.	0.08	Pt-Carbowax	0.035	39
$ZnT(C_{18})PyP$	–	EDTA	Red.		Pt-Carbowax	0.002	39
$ZnT(C_{18})PyP$	MV^{2+}	EDTA	Ox.		Pt-Carbowax	0.005	39
Acridine yellow	MV^{2+}	EDTA	Red.	0.56 (MV^+)	Pt, Pd	0.28	40
Acridine orange	MV^{2+}	EDTA	Red.?	0.16			41
$Ru(bpy)_3^{2+}$	MV^{2+}	EDTA	Ox.	0.11?	Pt-PEG	0.059	42
$Ru(bpy)_3^{2+}$	$Rh(bpy)_3^{3+}$	TEOA	Ox.	0.15	Pt	0.12	43
$Ru(bpy)_3^{2+}$	$Rh(bpy)_3^{3+}$	EDTA	Ox.	0.15	Pt	0.04	43
$Ru(bpy)_3^{2+}$	$Co(bpy)_3^{3+}$	Asc.	Red.		–	0.02	44
$Ru(bpy)_3^{2+}$	$Co(Me_2\text{-}bpy)_3^{3+}$	Asc.	Red.		–	0.13	44
ZnPcS	MV^{2+}	EDTA	Red.		Pt	10^{-4}	45
$Ru(bpz)_3^{2+}$	MV^{2+}	TEOA	Ox.	0.77			46
$Ru(bpy)_3^{2+}$	Ti^{3+}	–	Ox.		–	0.1?	47
Metal–sulfur chelates/THF		H_2O?	Red.		–	0.03 (267 nm)	48
					–	$< 10^{-5}$ (366 nm)	49
$Cr(Me_2\text{-}bpy)_3^{3+}$	–	EDTA	Red.		Pt	0.08 (pH 4.8)	50
$Cr(phen)_3^{3+}$	–	EDTA	Red.		Pt	0.002 (pH 4.8)	50
$Cr(Me_3phen)_3^{3+}$	–	EDTA	Red.		Pt	0.08 (pH 4.8)	50
$MgPc/DMSO\text{–}H_2O$	MV^{2+}	EDTA	Red.	0.47			51
$ZnTMPyP^{4+}$	MV^{2+}	EDTA	Ox.		Pt-PVA	0.06	52
$ZnTMPyP^{4+}$	MV^{2+}	EDTA	Ox.	0.9	Pt-Carbowax		53
$ZnTMPyP^{4+}$	–	EDTA	Red.		Pt-Carbowax		53
$ZnTPPS^{4-}$	MV^{2+}	EDTA	Ox.	$< 10^{-2}$	Pt-Carbowax	$< 10^{-3}$	53

photosystems is anticipated. For the same quenchers, amongst structurally similar complexes, [e.g. MV^{2+} quenching of cationic porphyrins, tetramethylpyridylporphyrinatozinc, $ZnTMPyP^{4+}$, and tetraaminophenylporphyrinatozinc, $ZnTAPP^{4+}$; $Co(sepul)^{3+}$ quenching of substituted bpy, phen complexes of Ru(II)], quite dramatic differences in ϕ_{cage} values (and hence ϕ_{H_2}) are observed, and at least part of these can be traced to the energetics and kinetics of photoredox reactions. Light-induced H_2 evolution studies in "sacrificial" three-component systems with catalysts are currently in a stagnant stage. Hence it is worthwhile reviewing the "state of the art" in the performance of each of the components.

Sensitizers

Water soluble porphyrins, such as $ZnTMPyP^{4+}$, have been the most efficient sensitizers to date, in terms of the spectral sensitivity to visible light excitation, cage escape yields and overall quantum yields for H_2 generation [5,37–39,52,53,62–66]. Amongst various metals, zinc, palladium and tin(IV) are the most efficient. With the most popular acceptor, methylviologen (MV^{2+}), ground state complexation of anionic water-soluble porphyrins (such as $TPPS^{4-}$) severely limits the efficiency of the photoredox processes, and hence their performance as sensitizers for H_2 evolution. The only exception has been from the work of Shellnutt [65] who reports efficient photoreduction of MV^{2+} with an octaanionic porphyrin, dihydroxytin(IV) uroporphyrin at pH 10. Unfortunately, at these alkaline pH values, most of the viologens (including MV^{2+}) are not capable of reducing water to H_2! We must point out an important factor that has to be kept in mind in designing systems for light-induced H_2 evolution. Because the redox catalytic steps (reactions such as (2) and (3)) are dark reactions with large overvoltages, at any given pH of the solution (acidic, neutral or basic) suitable sensitizer-relay systems where the S^* is capable of generating the appropriate relays (oxidants and reductants) which can take part in redox catalytic steps at the same pH must be found. Tuning the redox potentials of the relays to the solution pH is also essential. Though this is obvious, it appears to have been often overlooked. Phthalocyanines are structurally-related photosensitizers which are attractive for their light-harvesting capacity even in the red part of the solar spectrum. However, their performance (both as the neutral form and as sulfonatophthalocyanines) in sensitizing H_2 evolution has been very disappointing [45,51].

Transition metal polypyridine complexes are another class of sensitizers which have been widely studied. Earlier studies with substituted bpy and phen complexes of Ru, Rh and Cr have now been succeeded by a new series of bpy-analogs and diimine complexes with ligands such as bipyrazine, bipyrimidine, bipyridazine, biquinoline, bis(isoquinoline), (2-pyridyl)pyra-

zole, (2-pyridyl)quinoline, bi(benzimidazole), terpyridines, etc. [67–76]. With these it is now possible to tune the excited-state redox properties to a much wider potential range. Application of these new complexes to light-induced H_2 and O_2 evolution is yet to come. Polypyridine complexes of Cr and Rh lack even moderately intense absorptions of visible light, but upon excitation in the UV, they do act as true photosensitizers via reductive cycles [77–86]. Some of the Rh complexes are capable of acting as homogeneous catalysts for H_2 generation in the reduced forms (Rh(II) and Rh(I)) [79–86]. Similarly, heteropolyacids are an interesting group of polynuclear cluster complexes which have been shown to sensitize H_2 evolution in the UV via reductive cycles [18,21,27,87–89]. Quantum yields for H_2 generation with visible light, however, are very low ($\leqslant 10^{-3}$) mainly due to a lack of charge transfer character.

Acceptor relays

Undoubtedly, diquarternary bipyridinium, phenanthrolinium salts ("viologens") have been the favourite acceptor relays in all the model systems studied for several reasons [26,33,90–96]: tunability of redox potentials over a wide range by substitution (Table 3), high solubility in aqueous solutions, significant colour change between the oxidized and reduced forms, ease of reduction as well as ability to readily liberate H_2 from water in the presence of Pt group catalysts. In addition to their "poisonous" nature (they are used as the insecticide "paraquat"), extensive studies have revealed several other shortcomings of these compounds, such as their susceptibility to hydrogenation in the presence of Pt group metal catalysts, extreme sensitivity of the reduced form of viologens to the presence of oxygen, and also ease of formation of ground-state charge-transfer complexes with a wide variety of potential sensitizers and electron donor molecules.

Macro cage complexes of Co are new acceptors which are currently receiving careful scrutiny; early results with complexes such as $Co(sepul)^{3+}$ are very promising [23,28,97–100]. Sargeson et al. have shown the tunability of redox potentials in these compounds by subtle variations of the cage design [98,99]. Unlike other labile bpy or amine complexes of Co, these complexes have the attractive feature of being inert to substitution. (The labile nature of the polypyridine complexes as well as the tendency to form hydrides have been exploited in using them as homogeneous catalysts for H_2 evolution!) The cage escape yields of redox products in the electron transfer quenching of RuL_3^{2+} complexes are also quite high (0.3 to 1.0) [100]. Cobalticinium complexes have also been found effective as acceptor relays to mediate water reduction [18].
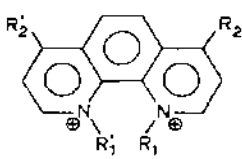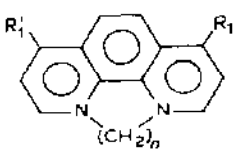
Electron donors

The number of electron donors found to be useful for the photoredox

systems under consideration has been very few—mostly amino acid derivatives and tertiary amines, especially EDTA and triethanolamine (TEOA). The irreversible decomposition of these donors upon oxidation is a very severe limitation of the system—hence the adjective "sacrificial". Repeated attempts to replace these by reversible donors (those that retain their chemical integrity during the redox cycles, e.g. Fe^{2+}) have met only very limited success. Reverse electron transfer and cross reactions plague the performance with reversible donors severely. The use of organized assem-

TABLE 3

Quaternary bipyridinium and phenanthrolinium salts for use as acceptor relays in water photoreduction systems [26,33,90–96]

Viologen	Abbreviation	$E_{1/2}$ (NHE)

Bipyridinium Salts

I	R_1	R_1'	R_2	R_2'	R_3	R_3'	R_6	R_6'		
Ia	Me	Me	H	H	H	H	H	H	MV^{2+}	−0.44
Ib	$PhCH_2$	$PhCH_2$	H	H	H	H	H	H	BV^{2+}	−0.34(−0.36)
Ic	$(CH_2)_2OH$	$(CH_2)_2OH$	H	H	H	H	H	H		−0.41
Id	Ph	Ph	H	H	H	H	H	H	PV^{2+}	−0.29
Ie	CN	CN	H	H	H	H	H	H		−0.29
If	Me	Me	Me	Me	H	H	H	H	$2TMV^{2+}$	−0.51
Ig	Me	Me	H	H	Me	Me	H	H	$3TMV^{2+}$	−0.83(−0.89)
Ih	Me	Me	Me	Me	H	H	Me	Me	HMV^{2+}	−0.59
Ii	Me	$(CH_2)_3SO_3^-$	H	H	H	H	H	H	MPV^+	−0.45
Ij	$(CH_2)_3SO_3^-$	$(CH_2)_3SO_3^-$	H	H	H	H	H	H	PVS^0	−0.40

	n	R_1	R_1'	R_2	R_2'	R_3	R_3'		
IIa	2	H	H	H	H	H	H	−0.38(−0.35)	
IIb	2	H	H	Me	Me	H	H	−0.50(−0.49)	
IIc	2	Me	Me	H	H	H	H	−0.48	
IId	2	H	H	H	H	Me	Me	−0.41	
IIIa	3	H	H	H	H	H	H	−0.65(−0.63)	
IIIb	3	H	H	Me	Me	H	H	−0.63(−0.56)	
IIIc	3	H	H	H	H	Me	Me	−0.55	
IIId	3	Me	Me	Me	Me	H	H	−0.77	
IVa	4	H	H	H	H	H	H	−0.64	

TABLE 3 (continued)

Phenanthrolinium Salts

	R$_1$	R$_1'$	R$_2$	R$_2'$		
Va	Me	Me	H	H		−0.51

	n	R$_1$	R$_1'$		
VIa	2	H	H		−0.25
VIIa	3	H	H		−0.18(−0.12)
VIIb	3	Me	Me	DMPP	−0.40
VIIc	3	Ph	Ph	DPPP	−0.31
VIId	3	Me	H	MPP	−0.22
VIIe	3	Cl	H	ClPP	−0.11
VIIIa	4	H	H		−0.45

blies helps to prolong the lifetimes of key intermediates so that even moderately-active catalysts take part. But unless very active catalysts which can selectively prevent the reverse electron steps can be found, the future for "sacrificial" systems does not appear very bright. It should be pointed out that irreversible decomposition of electron donors by itself is not always a severe limitation, for it can be used with advantage in several practical applications, such as cleaning of industrial wastes, etc. As will be seen later, with semiconductor dispersion systems as light absorbers, it is currently one of the most active areas of investigation.

Catalysts

The major thrust of activity in recent years has been in the identification and assay of heterogeneous catalysts of assorted types [101–113]. Colloidal systems have received special attention because in addition to providing extremely active high surface area catalysts, they enable a quantitative study of the efficiency of the photoredox and catalytic steps. The most commonly used is colloidal Pt and Rh sols prepared via chemical reduction of Pt(IV) or (VI) salts with citrate, hydrazine or $NaBH_4$. Excess reductant and ions are removed via dialysis and the naked Pt^0 sols protected against flocculation/coagulation by using inorganic or organic polymers such as

carbowax or polyvinylalcohol. Pt sols protected with carbowax are more stable and active than those protected with PVA. Alternatively, they can be deposited on solid supports, e.g. semiconductor oxide dispersions such as TiO_2 or zeolites. Pt/TiO_2, $Rh/SrTiO_3$, $Pt/Zeolite-Y$ are typical examples. (For semiconductor dispersions as support, bandgap illumination to photo-platinize the material in the presence of reductants such as acetate can also be used.) There have been several reports attesting the superior performance of Pt/TiO_2 (compared with colloidal Pt sols) both for their long-term performance (high turnovers) and for exhibiting near unity efficiency of redox catalytic steps. Section E provides an overview of the current understanding of the mechanism and kinetics of redox catalytic processes.

(ii) Photoproduction of O_2 from water

Progress in the design of photoredox systems for the generation of molecular oxygen from water has been much slower, partly because four electrons need to be transferred before O_2 formation can occur, whereas H_2 production requires only a two-electron storage. Polypyridine complexes and metalloporphyrins have been the main classes of sensitizers subjected to scrutiny, the latter especially because of their possible involvement in the natural photosynthetic machinery of green plants. Strangely enough, more definitive (positive!) results on the ability of the complex to sensitize O_2 evolution from water have been obtained with the former than with the latter. These are various possible reasons for this anomaly. One possibility concerns the inherent chemistry of these compounds, especially the location of redox potentials and chemical reactivity (stability) of oxidized sensitizer species. In polypyridine complexes, the redox potentials of successive oxidations–reductions are well separated from each other and thermal stability (especially to substitution reactions) is quite good in several of these redox states. In metalloporphyrins (especially closed-shell systems where the excited states have very long lifetimes and redox reactivity to participate in photoredox reactions), the redox reactions are π-system oxidations or reductions. The redox potentials are closely spaced ($\leqslant 200$ mV) facilitating disproportionation steps. This leads to the formation of dications which in the case of porphyrins are very susceptible to nucleophilic attack in aqueous media giving isoporphyrins.

Since the stability (inertness to substitution reactions or decomposition) and reactivity (towards redox catalytic steps) of photogenerated oxidants are the crucial limiting factors in determining the success of photochemical water cleavage systems, there has been extensive work (although much more is needed) on assessing the above two steps with several chemically-prepared oxidants and various redox catalysts (both homogeneous).

Thermal reduction of strong oxidants derived from the polypyridine complexes of transition metals such as Ru, Fe and Os, unassisted by catalysts, invariably leads to some decomposition (up to 10%) of the original tris complex into modified complexes whose spectral, redox and other chemical properties are similar to the original complex [114–131]. Only traces of O_2 are observed as a product though the yield increases somewhat at very alkaline pH with Fe and Os complexes. In addition, other products such as CO_2 (5–6 mol% with Ru) and free ligand bipyridine-N-oxide (with Fe) have also been observed. In all cases, the proposed mechanism of reduction involves some form of dissociated bpy, phen complexes where the coordination to the metal by one of the bpy N^- groups is replaced by OH^- (or water).

Fortunately, in the presence of assorted types of redox catalysts, retention of the chemical integrity of the tris(polypyridine) complexes is extremely good and under certain optimal pH conditions (dictated by the energetics—redox potentials of the metal complex and overpotentials for water oxidation on the catalyst material), near stoichiometric yields of O_2 are often observed. Thus, with good and active catalysts, the metal complexes can remain intact during several redox cycles and indeed the true catalyst-assisted oxidation of water to molecular oxygen can be observed [114–131] (Table 4). In photochemical systems, the turnover number with respect to the metal complex, though not in thousands (as has been observed with H_2-evolving systems) is still respectable.

Since there is always total reduction of the trivalent metal by water (or OH^-), irrespective of whether molecular oxygen is formed, and partial decomposition of the complex occurs whenever the redox catalysis is not effective (using the metal complexes as photoredox sensitizers), it is essential to find very efficient catalysts. Though Fe and Os polypyridyls also evolve O_2 from water in the presence of catalysts, due to lack of desirable excited state properties, $Ru(bpy)_3^{2+}$ and its analogs are the only transition metal polypyridine complexes that effectively serve as photosensitizers for water oxidation.

The situation with the use of metalloporphyrins in analogous experiments is not clear. A few years ago, we made detailed electrochemical studies of several water-soluble metalloporphyrins (especially Zn complexes of $TPPS^{4-}$ and $TMPyP^{4+}$) with and without redox catalysts present [132]. Subsequently, Porter et al. made similar studies on the same and similar metalloporphyrin systems [133–136]. For reasons which are not yet fully clear, in aqueous media controlled potential electrolysis (to yield monocations) is clean only with $TPPS^{4-}$ systems and not with those of $TMPyP^{4+}$. (The latter invariably yield isoporphyrins and like products.) With and without redox catalysts, the lifetime of $ZnTPPS^{3-}$ (monocation) is strongly pH dependent,

TABLE 4

Redox systems for the generation of molecular oxygen from water in the presence of redox catalysts

Sensitizer/oxidant	Catalyst	Optimal		Comments/results	Ref.
		pH	$[O_2]$ (%)		
$Fe(bpy)_3^{3+}$, $Fe(phen)_3^{3+}$	Hydroxocomplexes of Fe (?)			Dissociated complexes as intermediates; parallel paths yield ligand N-oxides and O_2 catalyzed by hydroxocomplexes of Fe	114
$Ru(bpy)_3^{3+}$	Co(II)	7.0	100	Co(IV) as catalytic intermediate	115
BrO_3^-	RuO_2/TiO_2	3.0	100	Br_2 and O_2 in stoichiometric yields	116
$M(bpy)_3^{3+}$ (M = Ru, Os, Fe)	–			Dissociated bpy complex as intermediate	117,118
Ce^{4+}	$RuO_2 \cdot H_2O$			Large surface area and low initial oxidant concentrations inhibit corrosion of RuO_2 to volatile RuO_4	119
Ce^{4+}	$RuO_2 \cdot xH_2O/TiO_2$		70	Optimal 7.5% RuO_2 loading, heat treatment 100°C, hydrated species are the active ones	120
$M(bpy)_3^{3+}$ (M = Ru, Fe, Os)	"RuO_2"	6.0 6.0 10.0	70(Ru) 25(Fe) 20(Os)	O_2 yields pH dependent	121 121 121
$Ru(bpy)_3^{3+}$	"RuO_2" PtO_2	3.0	90 10		122 122
Ce^{4+}	$[(bpy)_2(H_2O)_2Ru]_2O$ (oxo-bridged bpy-Ru dimer)			O_2 yields catalytic w.r.t. Ru dimer complex both in Ce^{4+} system and during electrolysis	123
Ce^{4+}	$[Ru(H_2O)(py)L_2]^{2+}$ L = 2(phenylazo)pyridine				

Oxidant	Catalyst	pH	Yield (%)	Comments	Ref.
M(bpy)$_3^{3+}$ (M = Ru, Fe, Os)	RuO$_x$–IrO$_x$/Zeolite Y-200	7.5	100(Fe)		125
		8.5	100(Ru)		125
		11.5	100(Os)		125
Fe(bpy)$_3^{3+}$, PbO$_2$, BO$_3^-$, Suprox(perisophthalic acid)	Colloidal RuO$_2$/SDS	9.0	100(Fe)	Colloidal RuO$_2$/SDS or PVP retains activity over six months	126
	RuO$_2$·xH$_2$O Colloidal RuO$_2$/PVP	7.0	100('')		126
M(bpy)$_3^{3+}$ (M = Ru, Fe)	Spinels (Co$_2$O$_4$, CoFe$_2$O$_4$, FeCr$_2$O$_4$, CoCr$_2$O$_4$) and M(OH)$_3$, M = Fe, Co, Cr, Al..		0–70		127
Ru(bpy)$_3^{3+}$	Co, Cu and Fe complexes with bpy, en, NH$_3$, EDTA..	10.0	10–70		128
Ru(bpy)$_3^{3+}$	Cr, Mn, Fe, Co... sulfo-phthalocyanines	9–10	5–65		129
Ru(bpy)$_3^{3+}$	Hydroxides of Fe, Co and Ni	6–8	91(Fe) 94(Co) 49(Ni)		130
Ru(bpy)$_3^{3+}$	Co$_{aq}^{2+}$	7.0	~100	[Ru^{3+}] = 0.01–1.0 mm, [Co^{2+}] ~ 0.1 Ru^{3+}, Co^{IV} as intermediate	131
Ce^{4+}, Ru(bpy)$_3^{3+}$	RuO$_2$/TiO$_2$ RuO$_2$//polybrene			Kinetics of reduction	131a
Ce^{4+}	RuO$_2$	~0	100		148

suggesting reactions with water (or OH^-). (For example, $t_{1/2}$ decreases from more than 1 hour at pH of approximately 4.5 to 20 min at pH 6.5 and a few minutes at pH 9.0.) In the presence of active RuO_2/TiO_2 catalysts, the Royal Institution group has recently obtained decent yields of oxygen from water upon photolysis of $ZnTPPS^{4-}$ with $S_2O_8^{2-}$. $ZnTPPS^{3-}$, like $Fe(bpy)_3^{3+}$, is a mild oxidant and hence evolves O_2 from water only at very alkaline pH [9]. $ZnTMPyP^{5+}$, on the contrary, is a much stronger oxidant, like $Ru(bpy)_3^{3+}$, ideal for use around neutral or acid pH. Unfortunately, electrochemical studies with this system have been ambiguous and photolysis studies with suitable electron acceptors controversial. The formation of $ZnTMPyP^{5+}$ in pulse radiolytic studies (oxidation with Br_2^-) is readily observed, and in the absence of catalysts the half-life is indeed quite long (several milliseconds, though not seconds or minutes), and its decay is enhanced markedly in the presence of colloidal redox catalysts such as RuO_2, in what appears to be a reaction with water. More detailed product analysis studies are required and such studies are currently under way in our laboratory and elsewhere.

Table 5 summarizes recent results on "sacrificial" systems that lead to light-induced oxygen generation from water [137–146]. For reasons similar to those elaborated for H_2-evolving systems, the useful acceptors have all been of "sacrificial" type (e.g. $Co(NH_3)_5Cl^{2+}$, $S_2O_8^{2-}$), i.e. they decompose to several products upon photoreduction. As with water electrolyzers and chlor-alkali electrolyzers, the heterogeneous catalysts of choice have been metal oxides especially RuO_2 and IrO_2. Several studies have established that "the hydrated" form of RuO_2, $RuO_2 \cdot xH_2O$, is the most active and this too is preferably used as a supported material such as RuO_2/TiO_2 or $RuO_2/Zeolite$ [119,120].

Catalysis of oxygen generation from water by RuO_2-based materials has initially been plagued by irreproducibility of the results obtained in different laboratories. Thus, in the first report [147] of RuO_2-catalyzed water oxidation by Ce^{4+} and $Ru(bipy)_3^{3+}$, the yield of oxygen observed was practically 100%. In subsequent studies Mills [148] and Shafirovich [121] found lower yields. Furthermore, an undesirable side reaction, i.e. the corrosion of RuO_2 to RuO_4, was detected. These controversial results led to a careful reexamination of the catalytic processes [119]. From a recent study [149], the key to the solution of the problem appears to be the pretreatment of RuO_2. Heating commercial $RuO_2 \cdot aq$ for several hours in air at 140°C provided highly active catalysts which gave practically reproducible 100% oxygen yield in the oxidation of water by Ce^{4+}. This very interesting observation indicates that the catalyst functions optimally at a rather narrow range in the degree of hydration of the RuO_2 surface, the presence of weakly-bound water favoring corrosion.

TABLE 5

Photoredox systems with redox catalysts for the oxidation of water to molecular oxygen

Sensitizer	Acceptor, (ϕ_{redox})	Catalyst	Optimal pH	[O₂] (%)	Comments/results	Reference
$Ru(bpy)_3^{2+}$	Eu^{3+}	RuO_2–Pt			H_2, O_2 yields catalytic but display a damped oscillatory behavior	137
	$S_2O_8^{2-}$	RuO_2/TiO_2	2.0		H_2, O_2 produced, $\phi(O_2) \sim 0.1$	138
	Prussian blue	Prussian blue (?)			Optimal 2% loading of RuO_2	139
	$S_2O_8^{2-}$	$RuO_2 \cdot xH_2O/TiO_2$				120
	$S_2O_8^{2-}$	Colloidal RuO_2/TiO_2			Flash conductivity studies, catalytic water oxidation occurs in a few ms	140
	$S_2O_8^{2-}$	"RuO_2"			$\phi(Ag^0)$ 0.04 (60% PEG) $\phi(O_2)$ 0.008 (80% PEG)	121
	Ag^+/PVA or PEG	RuO_2/Zeolite				141
	Mn^{IV} pyrophosphate	MnO_2	7.0	12–44	$\phi(Ru^{3+}) = 0.26$	142
	Mn^{IV} pyrophosphate	$Co(OH)_3$	7.0	70		143
	$S_2O_8^{2-}$	Hydroxides				
		of Fe, Co, Ni	8–9	34(Co)	$\phi(Ru^{3+}) = 0.77$	143
			8–9	36(Fe)		143
			8–9	9(Ni)		143
	$Co(NH_3)_5Cl^{2+}$	$RuO_2 \cdot xH_2O$ $CoCl_2$	4.8	21–25	Kinetic data on Ru^{3+} reduction; at ph 5, catalysis is by RuO_2 and at pH 5, by Co^{2+}	144
	$Co(NH_3)_5Cl^{2+}$	MnO_2	3.6	48		145
		RuO_2–TiO_2	4.7		Optimal at 10% RuO_2 loading	138
		RuO_x–IrO_x/ zeolite Y	4.5	100(16 h)		125
			4.5	25(4 h)		
		$[(bpy)_2(H_2O)_2Ru]_2O$ on clays (hectorite and sepiolite)			*trans* Isomer not active and *cis*	137
		"RuO_2"	4.5	20	slightly [O_2] pH dependent	121
$Ru(bpy)_3^{2+}$ / $Co(NH_3)_5Cl^{2-}$ / hectorite	$Co(NH_3)_5Cl^{2+}$	t-$[(bpy)_2(H_2O)_2Ru]$ on hectorite	4.2		Equal amounts of O_2, N_2	137
$Ru(bpy)_3^{2+}$	$Co(NH_3)_5Cl^{2+}$	Colloidal RuO_2	5.0		$\phi[O_2] = 0.03$	146
		$RuO_2 \cdot xH_2O$	5.0		$= 0.003$	146
		$CoSO_4$	5.0		$= 0.02$	146

As with the photoredox systems for H_2-evolution, an attempt to evaluate quantitatively the performance of the various photosystems in terms of quantum yields for the photogeneration of the water oxidant (ϕ_{redox}) and the efficiency of the redox catalytic steps (η_{cat}) can be made

$$\phi_{O_2} = (1/4)\phi_{redox} \cdot \eta_{cat} \tag{12}$$

There are certain optimal conditions under which oxidized polypyridyl metal complexes do oxidize water to O_2 with near stoichiometric yields in the presence of active catalysts (both heterogeneous, e.g. RuO_2, and homogeneous, e.g. Co^{2+}), i.e. η_{cat} is near unity for the dark reaction

$$4D^+ + 2H_2O \overset{cat}{\rightarrow} 4D + 4H^+ + O_2 \tag{13}$$

The kinetics of these dark reactions, however, are not as rapid as is the case with the oxidation of MV^+ on colloidal Pt. Similarly, the cage escape yields (ϕ_{redox}) in the oxidative quenching of sensitizers such as $Ru(bpy)_3^{2+}$ and $ZnTMPyP_4^+$ are quite high [$Ru(bpy)_3^{3+} = 1.0$ and 2.0 for quenchers $Co(NH_3)_5$, Cl^{2+} and $S_2O_8^{2-}$, respectively]. Thus, the oxygen quantum yields are anticipated to be around 0.25 or at least over 10% with inert sacrificial acceptors. Photolysis of systems $Ru(bpy)_3^{2+}$/acceptor/catalyst under steady state conditions, however, generate O_2 from water with quantum yields for O_2 at most a few percent! The ability to photosensitize O_2 evolution from water using visible light (even with low quantum yields) is certainly a significant step in the long and arduous march towards the goal of "complete" in vitro photosynthesis. Certainly the conditions (including a thorough understanding of the various redox reactions that follow light excitation of the sensitizer, identification of active redox catalysts and kinetics of the photoredox and catalytic steps optimized for the proper coupling of the two) must be optimized.

In all the photosystems studied, one possibility for the low ϕ_{O_2} is that the redox catalytic steps are not fast enough to regenerate rapidly the sensitizer in the (2 +) state. There is increasing evidence to indicate that $Ru(bpy)_3^{3+}$ itself has a substantial photochemistry of its own, that in the steady state the incoming photons (while they are wasted on one hand) actually lead the system into destructive pathways! Improper kinetic coupling of the two key steps is probably one of the reasons why most researchers (including ourselves) found only about 30% of stoichiometric yields of O_2 (stoichiometry with respect to the acceptor) after 1 to 2 h of photolysis of $Ru(bpy)_3^{2+}$/$Co(NH_3)_5Cl^{2+}$ in the presence of active $RuO_2 \cdot xH_2O$ catalysts. It required nearly 14 h of photolysis (at very low photon flux) by Lehn et al. to observe near stoichiometric yields of O_2.

D. PHOTODECOMPOSITION OF WATER IN HOMOGENEOUS SYSTEMS USING HOMOGENEOUS REDOX CATALYSTS

(i) Photoproduction of H_2 from water

Interest in the development of homogeneous catalysts which can assist liberation of molecular H_2 from water started with the early reports of Lehn et al. on $Ru(bpy)_3^{2+}/Rh(bpy)_3^{3+}/TEOA/PtCl_6^{4-}$ who found that appreciable amounts of H_2 was produced even in the absence of Pt salts [80,81]. Subsequently, UV photolysis of $Rh(bpy)_2Cl_2^+$ and $Rh(bpy)_3^{3+}$ in the presence of tertiary amines was also shown to produce H_2 [79]. With the known ability of Rh to form labile hydride intermediates, subsequent research included other hydride-forming systems such as Co complexes as potential candidates [22,29,44,82,150].

Homogeneous catalysis of H_2 and O_2 evolution from water is a very interesting and important area in studies of photochemical water cleavage for several reasons. One is the purely academic question: "how can one design photosystems that are capable of multi-electron storage and also use the charge equivalents to generate multi-electron transfer products such as molecular H_2 and O_2?", i.e. confer the relay and catalyst's functions on the same molecule (practically all known photoredox reactions involve discrete one-electron transfers, and occasionally one of the photoproducts undergoes subsequent dismutations involving electron transfer). The other major interest is that "homogeneous catalysts" can eliminate the need for large surface area heterogeneous catalysts whose deployment and recovery can be expensive.

Though the number of "homogeneous" catalyst-assisted systems which liberate H_2 or O_2 from water are numerous, only those involving Rh [79–85] and Co [22,29,44,150,153] complexes have been the subject of detailed mechanistic studies, especially by Sutin, Creutz, Hoffman, Shafirovich and coworkers. Homogeneous catalysis mechanisms are purely chemical involving several labile/reactive intermediates. Pulse radiolysis has in particular been extremely useful in identifying various intermediates, their spectra, redox and protolytic equilibria, and in elucidating their role in homogeneous catalysis.

Sutin et al. [29] propose two main types of redox cycles (homo- and heterosynthetic) which lead to H_2 evolution from water in systems that use Co complexes. (This, in fact, is based on earlier studies on hydridocobaloximes, where the mechanism of H_2 evolution has been shown to proceed via homolytic and heterolytic cleavage of the cobalt–hydrogen bond.) As in heterogeneous catalyst-assisted systems, the photoredox system initially generates a strong reductant (either via an oxidative or reductive cycle), and the

reduction potential of this is more negative than that for the H^+/H_2 couple. For homogeneous systems, there are additional constraints depending upon the nature of the water reduction pathway. In the homosynthetic pathway (eqns. (14–16)), the above condition that E^0 for the A/A^- couple is negative with respect to the H^+/H_2 potential again pertains, but with the additional
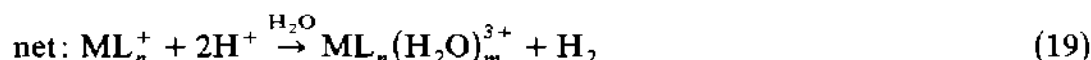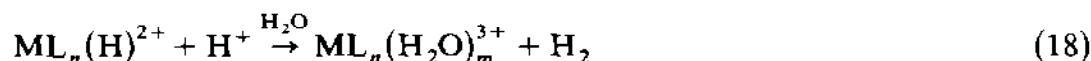
Homosynthetic route

$$ML_n^+ + H^+ \rightarrow ML_n(H)^{2+} \tag{14}$$

$$2ML_n(H)^{2+} \xrightarrow{H_2O} 2ML_n(H_2O)_m^{2+} + H_2 \tag{15}$$

$$\text{net: } 2ML_n^+ + 2H^+ \xrightarrow{H_2O} 2ML_n(H_2O)_m^{2+} + H_2 \tag{16}$$
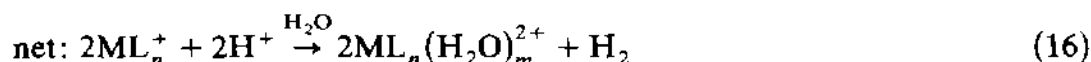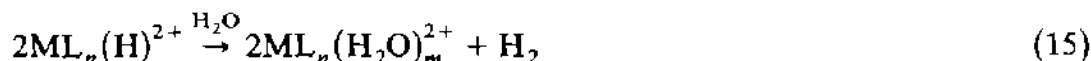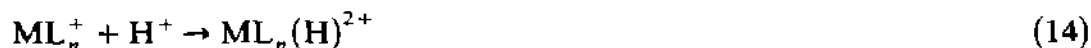
requirement that ML_n^+ have an accessible coordination site and that the hydride $ML_n(H)^{2+}$ be unstable with respect to M(II) and H_2.

For the homogeneous systems in which H_2 formation is heterosynthetic (eqns. (17–19)), the requirements are that E^0 for the A^+/A^- couple be

Heterosynthetic route

$$ML_n^+ + H^+ \rightarrow ML_n(H)^{2+} \tag{17}$$

$$ML_n(H)^{2+} + H^+ \xrightarrow{H_2O} ML_n(H_2O)_m^{3+} + H_2 \tag{18}$$

$$\text{net: } ML_n^+ + 2H^+ \xrightarrow{H_2O} ML_n(H_2O)_m^{3+} + H_2 \tag{19}$$

negative with respect to the H^+/H_2 potential, that ML_n^+ has an accessible coordination site and that acid-promoted decomposition of the hydride to give $ML_n(H_2O)_m^{3+}$ and H_2O occurs spontaneously. Both routes are thermodynamically favorable for the cobalt, with Co(II) being the product in both cases (eqn. (16)) in the homogeneous route and reaction (19) followed by the comproportionation reaction (20) in the heterogeneous route

$$ML_n^+ + ML_n^{3+} + 2ML_n^{2+} \tag{20}$$

With the Rh-bipyridyl systems, the mechanisms appear to be somewhat different. Although Rh(I) is photogenerated (in the absence of Pt) and at pH 7 is converted to a hydride, the analogues of the above sequences are not believed to occur since E^0 for the Rh^{III}/Rh^I couple lies positive with respect to the H^+/H_2 potential. In early reports, $Rh(I)(bpy)_2^+$ was postulated as a reactive intermediate for H_2 formation. In subsequent studies, it was concluded that $Rh^I(bpy)_2^+$ is not capable of generating H_2 by itself at appreciable rates in the "uncatalyzed" (without Pt) systems. There is an increasing consensus that a formal Rh(II) hydride, $RhH(bpy)_2^+$ (produced from the
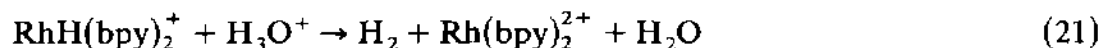
reaction of $RhH(bpy)_2^{2+}$ with $Rh(II)(bpy)_2^{2+})$ is a direct precursor of H_2. The following scheme provides a means of generating these intermediates, starting with excitation of $Ru(bpy)_3^{2+}$
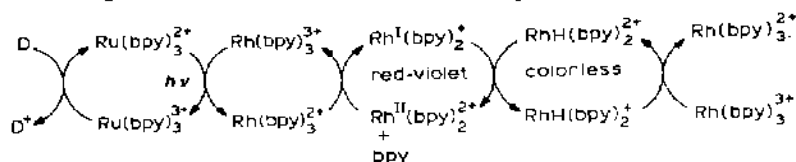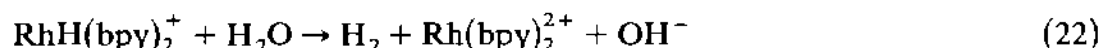

The generation of H_2 using $RhH(bpy)_2^+$ can occur from one or more of the following three reactions

(a) reaction with H_3O^+ in acidic aqueous solutions

$$RhH(bpy)_2^+ + H_3O^+ \rightarrow H_2 + Rh(bpy)_2^{2+} + H_2O \tag{21}$$

(b) reaction with H_2O in neutral aqueous solution

$$RhH(bpy)_2^+ + H_2O \rightarrow H_2 + Rh(bpy)_2^{2+} + OH^- \tag{22}$$

(c) bimolecular reactions

$$2Rh(bpy)_2^+ \rightarrow H_2 + 2Rh(bpy)_2^+ \tag{23}$$

Heteropolyacids are the other class of compounds recently studied which spontaneously liberate H_2 from water upon photolysis in the presence of suitable electron donors (e.g. alcohols). The interesting feature of these is that they can act as multi-electron storage devices as do colloidal metal sols. The quantum yields for H_2 production with UV light are respectable (a few percent at best in "uncatalyzed systems" and about 0.1 with Pt catalysts). But, as we mentioned earlier, their visible light response is quite low.

It is readily seen that in all of the homogeneous systems, the overall gas evolution from water is the result of a delicate balance of equilibria and rates for sometimes as many as twenty equations. In the presence of heterogeneous redox catalysts which can intervene in some of the very early steps, the reaction sequences that lead to molecular H_2 or O_2 are greatly simplified. Often this is accompanied by an increase in the overall product quantum yields (i.e. the product quantum yields approach close to the redox yields of primary/key intermediates), as has been observed with the introduction of Pt catalysts in systems using Rh-polypyridyls and heteropolyacids.

(ii) Photoproduction of O_2 from water

Attempts to catalyze water oxidation to give molecular oxgen using various metal ions and complexes have a long history. Early interests were related to the "possible role of manganese ions in the water-splitting act of green plant photosynthesis". For several decades, there was an intense interest (which still persists) in designing "in vitro" systems for water

oxidation using various Mn complexes (also to some extent Co and Fe complexes), especially in the groups of Calvin, Porter, Shilov, Sawyer, to name but a few. The Mn compounds examined spanned a wide range: simple Mn ions, MnO_2, MnO_4^-, Mn-polypyridyls, Mn porphyrins, Mn phosphates, Mn phthalocyanines, etc. [151]. Sometimes, there were positive reports on water splitting which later became controversies.

Almost a decade ago, Creutz and Sutin proposed the use of $Ru(bpy)_3^{3+/2+}$ couple as a potential relay species to mediate water oxidation [152]. It was reported that upon alkalization of acid-aqueous solutions of $Ru(bpy)_3^{3+}$ to about pH 9, copious evolution of O_2 from water (about 80% of the stoichiometry dictated by the equation (24))

$$Ru(bpy)_3^{3+} + OH^- \rightarrow Ru(bpy)_3^{2+} + 0.5\ H_2O + 0.25\ O_2 \qquad (24)$$
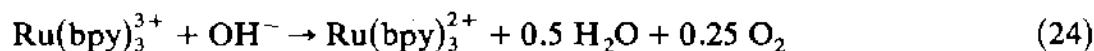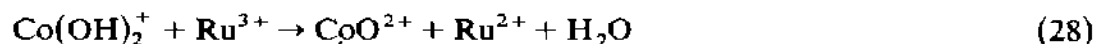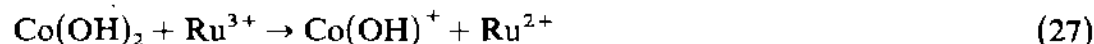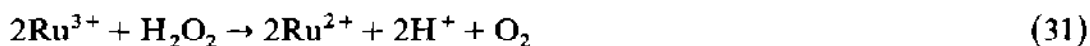
was observed. Subsequently, it was found that in carefully purified samples, the $[O_2]$ was $< 10\%$ over a wide range of pH, but O_2 yields increased markedly with the addition of very low quantities of metal ions such as Co^{2+} and Fe^{3+} [130,131,153,154]. Hydroxo complexes of metal ions were suspected to be potential intermediates. Recently, these results were supplemented by the observations by Meyer, Chakrovarthy et al., that oxo/hydroxo complexes such as $[Ru(IV)(py)L_2]^{2+}$, $[(bpy)_2(H_2O)_2Ru]O^{4+}$ catalyze efficiently O_2 evolution from water in reactions using Ce^{4+} as an oxidant [123,124]

$$4Ce^{4+} + 2H_2O \xrightarrow[\text{complexes of Ru}]{\text{oxo/hydroxo}} 4Ce^3 + O_2 + 4H^+ \qquad (25)$$
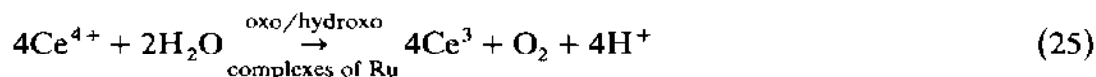
In the past few years, several groups have confirmed the beneficial effects of metal ions (hydroxo/oxo complexes) to catalyze O_2 evolution from water. Thus, all these developments have now rekindled the earlier hopes that it is possible to efficiently catalyze O_2 evolution with suitable homogeneous catalyst systems.

O_2 evolution from water using $Ru(bpy)_3^{3+}$ as a sensitizer, $Co(NH_3)_5Cl^{2+}$ or $S_2O_8^{2-}$ as sacrificial acceptors, and $Co(OH)^+$ as catalyst has been the only system that has been well studied. Based on detailed kinetic studies, the following mechanism involving Co(IV) and H_2O_2 as key intermediates has been proposed [115,131] (eqns. 26–31)

$$Co^{2+} + 2H_2O \rightarrow Co(OH)_2 + 2H^+ \qquad (26)$$

$$Co(OH)_2 + Ru^{3+} \rightarrow Co(OH)^+ + Ru^{2+} \qquad (27)$$

$$Co(OH)_2^+ + Ru^{3+} \rightarrow CoO^{2+} + Ru^{2+} + H_2O \qquad (28)$$

$$CoO^{2+} \rightarrow Co^{2+} + H_2O_2 \qquad (29)$$

$$CoO^{2+} + Co^{2+} \rightarrow CoOCo^{4+} \rightarrow \text{``}Co_2^{III}O_3\text{''}_{(s)} \qquad (30)$$

$$2Ru^{3+} + H_2O_2 \rightarrow 2Ru^{2+} + 2H^+ + O_2 \qquad (31)$$

$$\left[Ru^{3+} = Ru(bpy)_3^{3+}\right]$$

The side reaction (eqn. 30) has been introduced to account for the production of Co_2O_3 or a related solid formed when the concentration of $Ru(bpy)_3^{3+}$ and Co^{2+} are comparable and the O_2 yield greatly diminished under these conditions.

The Co(IV) product has been pictured as the "yl" CoO^{2+} by analogy with other M(IV) species. In general, the catalysis proceeds through outer-sphere one-electron oxidations to produce Co(IV). Depending on the pH and the nature of the oxidant, different steps in the sequence may become rate determining. For example, with oxidants stronger than $Ru(bpy)_3^{3+}$ or for $Ru(bpy)_3^{3+}$ at higher pH, the peroxide formation could become rate limiting. The last reaction, i.e. decomposition of H_2O_2 by transition metal ions and complexes, is a well-known thermal reaction. The mechanism of catalysis with the Ru complexes mentioned earlier, e.g. $[(bpy)_2(H_2O)_2Ru(III)]_2O^{4+}$, presumably occurs by analogous paths. Ru(IV) or higher oxidation states can fulfil the role of Co(IV) (the site of O–O bond formation). The formation of highly oxidizing "yl" ion (CoO^{2+}, RuL_2pyO^{2+} etc.) thus appears to be a feature common to the homogeneous catalysts presently known.

A recent result from our laboratory [155] illustrates that relatively subtle chemical changes in the bipyridyl-ligand of $Ru(bpy)_3^{2+}$ can have drastic effects on the water oxidation reaction. Thus, substitution in the 4,4′ position of all bpy-ligands by carboxylic acid groups produces a 300 mV increase in the redox potential of the Ru(II)/Ru(III) couple. As a consequence, tris(2,2′-bipyridine-4,4′-dicarboxylic acid) ruthenium(III) is capable of generating oxygen from water, even at pH < 0. Interestingly, this reaction proceeds also in the absence of a RuO_2 catalyst. Electrochemical studies [155] show that an autocatalytic reaction mechanism is likely to be operating. Part of the oxidized complex undergoes a chemical change (presumably the loss of one bipyridyl ligand) producing a homogeneous water oxidation catalyst. The nature of this catalytic species is presently being investigated.

E. HETEROGENEOUS REDOX CATALYSIS IN PHOTOCHEMICAL WATER CLEAVAGE: PRINCIPLES, MECHANISMS

A recurring theme in all the discussion so far has been that the ability of photogenerated oxidants and reductants to reduce or oxidize water to molecular hydrogen or oxygen spontaneously is very poor, and that it is greatly facilitated if redox catalysts of the homogeneous or heterogenous type are introduced. In the preceding section, it was shown that in homoge-

neous catalysis, most often the operative mechanisms are purely chemical involving formation and decomposition of several protic redox equilibria. In this section, we will address ourselves to the mechanisms and kinetics of heterogeneous catalysis as applicable to photochemical water cleavage.

What is expected from heterogeneous redox catalysts? Obviously, as multielectron transfer catalysts they should be capable of accumulating charges or at least have sites where a sequence of reactions can occur giving rise to the overall gaseous products with some built-in mechanisms for the regeneration of the catalytic surfaces after each cycle. This requirement is analogous to that cited earlier for homogeneous catalysts, but heterogeneous catalysis being a surface phenomenon, the nature of the catalyst surface plays a crucial role. In the choice of materials, the principles of electro-catalysis are obvious guides, i.e. those catalytic materials are used for which the overvoltage requirements for the desired reactions are low; examples are the Pt group metals for the H_2 evolution reaction and the so-called "dimensionally-stable anodes" composed of RuO_2 supported on Ti (or TiO_2) for O_2 and Cl_2 evolution reactions. Actually, it is the excellent performance of various electrocatalytic materials in water photolysis systems—as finely divided particles instead of macroelectrodes—which has led to the conclusion that the mechanism of action of heterogeneous catalysts are simply that of miniature electrodes or "microelectrodes".

According to this electrochemical model, the reducing radicals such as MV^+ impose their potentials on the Pt particle, and the cathodically-polarized particle subsequently proceeds to carry proton reduction to H_2. The behavior of the particle is very much that of a macroelectrode. It provides a medium by which the number of electrons (or equivalents) of two-half reactions can be matched

$$MV^+ \xrightarrow{Pt} MV^{2+} + e^- \tag{32}$$

$$e^- + H^+ \xrightarrow{Pt} 0.5\,H_2 \tag{33}$$

It also provides a surface for the lowering of the activation energy of one or both of the coupled half-cell reactions. As the particle acts simultaneously both as a cathode and anode, in the steady state they assume a "mixed potential", and the current corresponding to this potential represents the rate of H_2 evolution on the catalyst particle. Analogous anodic polarization of the catalyst particles by the impinging oxidant molecules would explain the performance of the oxidation catalysts.

From a quantitative analysis of this model, in terms of current–potential curves of the coupled reactions, it is possible to predict the behavior of the system under various experimental conditions. Thus, from an analysis of the overlap (intersection) of the anodic and cathodic curves, experimental results

on the effect of pH, effect of relay redox potential, influence of the nature of the electrode material, effect of the particle size, etc., are all quantitatively explained. The reader should consult earlier reviews [8,156] and also original publications in this area, especially the work of Spiro, McLendon and Albery, for details [157–164].

As the interest in catalyst-assisted photoredox processes continues to grow, several physical methods are being adopted for the characterization of catalyst particles and films (AAS (atomic absorption spectroscopy), ESCA and Auger spectroscopy, TGA, DTA, BET, etc.) and for the study of catalytic processes (pulsed methods such as laser photolysis and pulse radiolysis, stopped flow kinetics, electrochemical methods such as cyclic voltammetry and photoelectrochemical cells involving catalytic electrodes and particles). Extensive discussions on these techniques and their applications can be found in a review article published elsewhere [156]. Here, we restrict ourselves to outlining some general features.

A useful feature of the finely divided (colloidal) catalysts is their optical transparency to most of the visible light, and hence laser photolysis and pulse radiolysis methods are ideally suited for the study of the kinetics of coupled redox reactions occurring on the catalyst particle. The method consists of generating in a very short time (< 20 ns) the water oxidant or reductant with the aid of a laser or a 2 MeV electron pulse and following by optical adsorption or by conductivity the growth and decay of redox species in the presence and absence of catalysts. Thus, the method has been applied successfully both for the oxidation reactions (oxidation of MV^+, benzophenone ketyl, $(CH_3)_3CÖH$ radicals on colloidal Pt, Au, Ag, etc.) as well as reductions (reduction of $Ru(bpy)_3^{3+}$, $ZnTMPyP^{5+}$ on colloidal RuO_2/TiO_2). Reaction order and rate constants measured under various conditions provide information about the charging and discharging reactions on the colloidal catalyst. Analysis of rate data obtained at various Pt particle size and concentration in terms of Smoluchowski's equation show that for example MV^+ reaction on Pt is indeed diffusion-controlled.

Pulse radiolysis also provides an elegant method for the radiolytic preparation of colloidal metal sols. Henglein, Meisel and others have exploited the technique to generate active colloidal sols of Pt, Ir, Ag, Au and Cd and have obtained elegant results on the electron storage capacity of colloidal metal sols which correlate well with the known overpotential characteristics of these metals. Estimates for the electrical storage capacity, C, of colloidal particles per liter of the solution are 0.98, 0.94 and 0.40 Farad l^{-1} for Ag, Cd and Au sols, respectively. This implies that Ag particles can carry about 450 electrons in the steady state but due to the rapid reduction of charges to H atoms on Au, this number is reduced to about 39.

Stopped flow kinetics is a "sister" technique to study the kinetics of redox

catalytic reactions. Here the chemically-preprepared oxidants and reductants are rapidly mixed with the catalyst solution and the disappearance of the relay species monitored spectrophotometrically. Due to the inherent limitations on the rapidity with which two solutions can be mixed, the technique is ideally suited for the study of slow thermal (dark) catalytic reactions occurring over several milliseconds. As with the pulse photolysis/radiolysis methods, both water oxidation and reduction using catalysts have been studied.
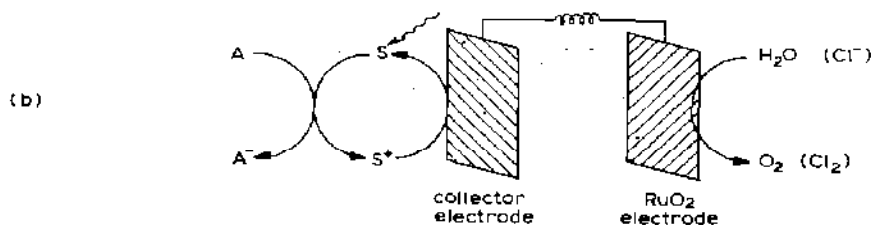
Instead of using chemically pre-prepared oxidants or reductants, an electrode can be used, and by single sweep and cyclic voltammetry of the relay species with and without catalyst presence the kinetics of the redox catalytic steps can be followed. Both MV^{2+} and $Ru(bpy)_3^{2+}$ have been studied in the presence of colloidal Pt and RuO_2, respectively. The rate constant data measured by electrochemical methods are, in general, in good agreement with those obtained from independent laser photolysis, pulse radiolysis or stopped flow mixing results.

Heterogeneous catalytic reactions that follow photoredox processes in dye-based systems can also be mimicked in appropriate photoelectrochemical cells involving catalytic (Pt or RuO_2) macroelectrodes. An advantage of cells of the type shown is that they allow a closer visualization of the heterogeneous catalyst function as "microelectrodes". From the individual $i-E$ curves for the illuminated compartment and the dark compartment, it is

Photoelectro (synthetic) cells for H_2: $[C/EDTA, Ru(bpy_3^{2+}, MV^{2+}//H_2O/Pt]$

(a)

collector electrode   Pt electrode
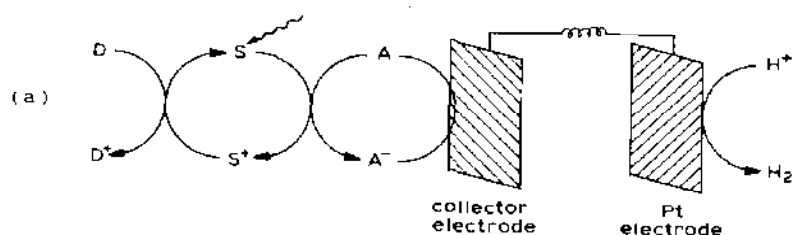
Photoelectro (synthetic) cells for O_2 (Cl_2): $[C/S_2O_8^{2-}, RuL_3^{2+}//H_2O/RuO_2]$

(b)

collector electrode   RuO₂ electrode

possible to predict directly the efficiency (photocurrent and potentials) for

the photoelectrochemical cells. For identical collector and counterelectrodes, this corresponds to the partial current (H_2 or O_2 rate) and the mixed potential at the catalyst particle. Studies of photoelectrochemical cells of the above type also enable a better understanding of the factors such as electrode size, selectivity and mass transport restrictions that control the performance of photogalvanic cells on the one hand, and product-generating photoelectro(synthetic) cells on the other.

F. WATER CLEAVAGE AND PHOTOCATALYSIS BY UV AND VISIBLE LIGHT IN SEMICONDUCTOR BASED SYSTEMS

(i) Water photolysis using semiconductor dispersions

In recent years, the main thrust of research has been in the application of semiconductor-based microheterogeneous systems to split water photochemically into hydrogen and oxygen. UV light-induced water decomposition will be discussed first. Most of the work in this field has concentrated on wide bandgap semiconductors such as TiO_2 or $SrTiO_3$ loaded with noble metal catalysts. Excitation of the semiconductor by ultraviolet light generates electron hole pairs (eqn. (34))

$$TiO_2 \xrightarrow{h\nu} TiO_2(e_{cb}^- + h^+) \tag{34}$$

The electrons are trapped by the noble metal deposit, e.g. Pt, where hydrogen is subsequently evolved

$$2e_{cb}^- + 2H^+ \xrightarrow{(Pt)} H_2 \tag{35}$$

The concomitant hole reaction involves oxidation of water to oxygen

$$4h^+ + 2H_2O \rightarrow O_2 + 4H^+ \tag{36}$$

The first study of this type was published by Bulatov and Khidekel [165] who reported that acidic aqueous dispersions of TiO_2 loaded with Pt decompose water under bandgap irradiation. Numerous other investigations followed [166–185] and these have been reviewed [5,16]. More recently, this field, together with visible light-induced water cleavage, has unfortunately become the subject of controversy and polemic. In part, this is due to the fact that there were problems with the reproducibility of the preparation of catalysts in different laboratories. The controversy mentioned above concerning the suitability of RuO_2 as water oxidation catalyst is a typical example. In addition, it became apparent that the simple sequence of reactions (34) to (36) could not account for all the experimental observations. In particular, during photolysis of water in closed systems, there is frequently only hydrogen evolution observed, and no or very little oxygen is released in the gas phase [184–187]. This has led to the postulation that the

hydrogen observed arises from the oxidation of Ti^{3+} ions present in the TiO_2 particles [186] or that there is anodic oxidation of carbonaceous impurities. In our earlier investigations [188], we had attributed lack of oxygen generation to the photo-uptake of O_2 via reduction by conduction band electrons of TiO_2. Recent water photolysis experiments with TiO_2 particles loaded with Pt or Rh have provided ample confirmation of this hypothesis [184, 185,187,189–192]. Using redox indicators such as permanganate or o-dianisidine [191], it could be unambiguously shown that peroxo- or superoxo species were formed during O_2-photo-uptake and also as the anodic reaction product during photolytic reduction of water to hydrogen. In contrast to materials such as ZnO, where photo-uptake of oxygen leads to the formation of free hydrogen peroxide in solution, in the case of TiO_2 the peroxide is associated with the solid [184,189–194]. According to a recent study [194], the capacity for peroxide uptake by TiO_2 (anatase) is as high as 20 molecules H_2O_2/nm^2 surface area. It is worth mentioning that apart from oxygen reduction by conduction band electrons, peroxides can also be produced via the oxidation of surface OH-groups by valence band holes. Investigations are presently undertaken to determine the detailed mechanism of peroxide formation as well as the structure of the peroxo complex associated with the TiO_2 particles. Very likely, μ-peroxo titanium dimers are the prevailing species and their formation has been shown to occur via valence band hole pairing in other oxides such as MgO [195].

The fact that in titania-based water cleavage systems peroxide can be produced in the anodic reaction instead of oxygen is advantageous since it opens up a way to overcome the H_2/O_2 separation problem which is inherent to microheterogeneous energy conversion devices. However, there is also a disadvantage which arises from the inhibitory effect of the peroxide on the water cleavage activity of the catalyst during the photolysis, as H_2 and peroxide accumulate in the system. Fortunately, a striking improvement of the performance of the system is achieved by addition of Ba^{2+} ions to the solution [193]. We attribute the promoting effect of barium ions to the formation of insoluble barium peroxide. The solubility product of BaO_2 is so small ($K = 10^{-17.5}$) [197] that Ba^{2+} can act as a peroxide scavenger. In this way, peroxide is removed from the systems allowing the catalyst to operate at higher efficiency.

Water cleavage systems that produce peroxides instead of oxygen would be without value for the solar generation of hydrogen if no methods could be found to decompose these peroxo-species in a simple and complete fashion. It was found earlier that prolonged flushing of the TiO_2 dispersion with an inert gas such as Ar or nitrogen affords already at least partial decomposition [184–186]. However, once the hydrogen evolution curve approaches the plateau region, it is no longer possible to regenerate entirely

the initial catalytic activity by this procedure [184,186]. A very important observation was made in our laboratory during studies of the TiO_2/Pt dispersions containing barium ions. It was found that heating the catalyst for a few hours at 200–300°C under nitrogen restored entirely its initial water cleavage activity. Apparently, exposing the catalyst to elevated temperature leads to complete decomposition of the peroxo-species formed concomitantly with hydrogen. If the decomposition temperature could be lowered further, e.g. by using appropriate catalysts, the formation of peroxides could well be tolerable, and even desirable in applied systems, where it would present a viable solution to the hydrogen–oxygen separation problem.

While peroxide is the likely oxidation product from water photolysis in TiO_2 particulate systems, concomitant formation of near stoichiometric amounts of oxygen and hydrogen has been observed in special cases. These comprise high temperature and low pressure conditions during irradiation, the use of gaseous instead of liquid water [196], open systems where an inert gas is bubbled through the solution and the use of bifunctional catalysts [178,197–199]. In the last case, ruthenium dioxide is loaded in addition to Pt on to the TiO_2 particles. So far the role of RuO_2 has not been entirely clarified. On the one hand, it could promote transfer of holes from the valence band of the semiconductor to water, and this has been established unequivocally for visible light-induced oxygen evolution on CdS particles [200]. On the other hand, when TiO_2 is used as a support, RuO_2 could also act as a catalyst for the decomposition of peroxides, since holes can also be trapped by surface OH groups.

Investigators who irradiate semiconductor dispersions in liquid water at room temperature in a closed flask should as a rule not expect any significant accumulation of O_2 in the gas phase since the catalyst employed for hydrogen generation, e.g. Pt, promotes oxygen reduction to peroxide at the same time. These considerations apply also to visible light-induced water cleavage devices where apart from reduction at the hydrogen evolution catalyst, oxygen is also removed by reaction with electron relay species such as MV^+. The newcomer to this field should be alerted, in the analysis of small amounts of oxygen, to the various pitfalls which have been discussed in ref. 200. For example, the conventionally applied chromatographic technique where gas is sampled from the headspace above the irradiated solution through a septum can give misleading results. Oxygen diffusion through the septum may occur more rapidly than that of nitrogen leading to accumulation of O_2 in the gas phase. Experiments with $^{18}O_2$-labelled water, as performed for example in our recent analysis of light-induced oxygen generation in CdS dispersions [200], are probably best suited to remove doubts about the origin of O_2 in these systems and to avoid misinterpre-

tation of the results. In the event that the investigator, who performs water photolysis with a titania-based catalyst in a closed system, observes the appearance of H_2 but not O_2 in the gas phase, it is likely that peroxo- or superoxo-species are formed in the anodic part of the water splitting reaction. The alternative suggestions that organic impurities or Ti^{3+} ions serve as sacrificial electron donors in these systems can be readily excluded by determining the carbon and Ti^{3+} ion content of the catalyst. For the latter analysis, ESR and colorimetric [201] techniques are available.

For solar application, it is crucial to shift the wavelength response of the light absorber into the visible. So far, three different strategies have been tested. The first involves the use of semiconductor particles with smaller bandgap than TiO_2. Apart from a recent report [197] on colloidal V_2O_5, bandgap 2.7 eV, these studies have concentrated on CdS particles [5] as light-harvesting units. In this case, it becomes mandatory to use a highly active oxygen-evolution catalyst, such as RuO_2 or Rh_2O_3, to promote water oxidation by valence band holes and suppress photocorrosion. Photoinduced oxygen uptake is an undesirable side reaction in this system since it leads to the oxidation of CdS giving $CdSO_4$ [202]. As was suggested by Harbour et al. [203], this reaction is expected to occur also in water cleavage systems when the photolysis is performed in a closed vessel without intermittent removal of gaseous products, and it would lead to the destruction of the semiconductor. A very important paper published recently deals with simultaneous hydrogen and oxygen evolution in dispersions of colloidal cadmium sulphide loaded with RuO_2 and another noble metal [338].

Chromium doping of TiO_2 has been attempted to shift its wavelength response in the visible. The problem with these particle preparations so far has been long-term stability. Relatively high temperatures (at least 800°C) are required to introduce Cr ions into the TiO_2 lattice. Unfortunately, under these conditions, chromium catalyzes the transformation of anatase into rutile. Since TiO_2 (rutile) particles are unsuitable for water cleavage, this transition must be avoided by doping at lower temperature, i.e. 400°C. However, Cr-doped colloidal TiO_2 particles prepared in this fashion release Cr ions in the aqueous solution and thereby lose their visible light response.

The third approach to split water by visible light involves dye sensitization, and this has given very promising results so far. In practically all cases $Ru(bipy)_3^{2+}$ or related chromophores served as sensitizers. These were used in conjunction with two redox catalysts, i.e. Pt and RuO_2, to promote water reduction and oxidation, respectively. An exception is the Prussian blue-catalyzed system of Kaneko et al. [206]. It is advantageous to use titania as a catalyst support since the TiO_2 particles are able to serve as oxygen carriers, as has been discussed. This allows the water cleavage reaction in closed systems to be sustained. However, clay-supported catalysts (again a combi-

nation of Pt and RuO_2) have also been employed in conjunction with $Ru(bipy)_3^{2+}$ as a sensitizer [207].

Apart from particulate dispersions, membrane-based systems are becoming increasingly important. In this context, attention is drawn to a recent patent by the Toshiba Corporation [208]. This system uses a TiO_2 membrane loaded on one side with Pt and on the other with RuO_2. A $Ru(bipy)_3^{2+}$ derivative is used as a sensitizer and is attached to the RuO_2 side of the membrane. Light-induced charge injection is followed by electron migration to the Pt side where hydrogen is evolved. The $Ru(bipy)_3^{3+}$ complex evolves oxygen from water, the reaction being promoted by the colloidal RuO_2 catalyst [209]. A similar approach has been published by Velasco [210] who employed a Nafion membrane to separate the same two catalysts. In his case, light was absorbed by a combination of two sensitizers $Ru(bipy)_3^{2+}$ and $Ru(bipyrazyl)_3^{2+}$, and the electron was transported across the membrane by a viologen-type carrier.

In earlier studies [178] $Ru(bipy)_3^{2+}$ or a surfactant derivative was used as a sensitizer and in some cases methyl viologen was added as electron acceptor. These were used in connection with an industrially-developed catalyst consisting of amorphous oriented anatase particles loaded with Pt and RuO_2 [211]. Initial results were promising [178]; however, the reproducibility of catalyst preparation, in particular the method of loading with Pt, turned out to be a problem. Conventional exchange or impregnation procedures could not be applied since it was important to avoid exposing the TiO_2 support to high temperatures which would have decreased its surface area and degree of hydroxylation. Both properties were found to have a crucial influence on water cleavage activity. An attempt to reproduce the earlier results with a similar catalyst [199] yielded hydrogen and oxygen generation under UV-light excitation, while the quantum yield of H_2 evolved in the visible was very small ($\phi \sim 10^{-4}$).

Over the last few years, it has been possible to develop more reliable systems which afford water cleavage by visible light by improving both the type of sensitizer employed and the catalyst preparation. A new and exciting development in this area has been the sensitization of TiO_2 by surface derivatization with transition metal complexes [335]. For example, irradiation of acidic (pH 2) solutions of RuL_3^{2+} $2Cl^-$ (L = di-isopropyl-2,2'-bipyridine-4,4'-dicarboxylate) in the presence of TiO_2 at 100°C leads to the loss of one bipyridyl ligand and the chemical fixation in the RuL_2^{2+} fragment at the surface of the TiO_2 particles through formation of Ru–O–Ti bonds. These surface complexes are very stable and shift the absorption onset of TiO_2 beyond 600 nm. The reflectance spectrum exhibits, apart from the bandgap transition of TiO_2 below 400 nm, a pronounced adsorption in the visible with a maximum at 480 nm and a tail extending beyond 600 nm.

The features in the visible resemble closely those observed for cis-Ru(bipy)$_2$(H$_2$O)$_2$ adsorbed on to hectorite [212] and are therefore attributed to cis-RuL$_2^{2+}$, chemically linked to the TiO$_2$ particles via one or two oxygen bridges.

RuL$_2^{2+}$-derivatized TiO$_2$ particles loaded with RuO$_2$ and Pt are active in producing hydrogen from water by visible light in the absence of a sacrificial organic donor. Illumination at 100°C of 50 mg of catalyst dissolved in 40 ml H$_2$O (pH 2, HCl) with $\lambda > 420$ nm light resulted in the formation of H$_2$ with an initial rate of 30 μl/h. Typically, 400 μl of H$_2$ were produced during 20 h of irradiation. The catalyst maintained its activity over at least two weeks of photolysis at 100°C during which it was exposed to various pH conditions and repeatedly washed with water and centrifuged. The total amount of H$_2$ produced corresponded to a turnover number of 80 with respect to RuL$_2^{3+}$. We have also observed O$_2$ generation during photolysis at 100°C, and injection of 400 μl gas sampled after 12 h of irradiation showed that 240 and 120 μl H$_2$ and O$_2$, respectively, were produced. Oxygen appearance in the gas phase was not consistently observed, however. In particular, at lower than boiling temperatures, only H$_2$ was found. We attribute this effect to photo-uptake of O$_2$ by the TiO$_2$ particles and have obtained evidence for the occurrence of such a process by peroxide analysis as described in ref. 197.

Thus a new technique of chemical derivatization of TiO$_2$ with ruthenium bipyridyl derivatives to shift its wavelength response in the visible has been introduced. Sensitization is made particularly effective by introducing the semiconductor surface directly into the coordination sphere of the transition metal complex. Similar derivatization may have inadvertently played a role in our earlier water photolysis studies with RuL$_3^{2+}$ using bifunctional TiO$_2$/RuO$_2$/Pt as redox catalyst [188]. Apart from efficient electron injection, RuL$_2^{2+}$ belongs to a class of complexes comprising molecules such as Ru(bipy)$_2$(H$_2$O)$_2^{2+}$ or its dimer which are known to be catalysts for a series of important reactions, such as water oxidation [123,124], or chlorine generation from chloride [213]. These processes are presently being investigated in detail.

(ii) Catalyst-assisted photoprocesses on semiconductor electrodes

The utilization of redox catalysts to promote multi-electron transfer processes is not restricted to homogeneous dye-based and semiconductor particulate systems, but is finding increasing application in photoelectrosynthetic cells incorporating semiconductor electrodes. It has been known for quite some time that p-type semiconductors are poor electrocatalysts for H$_2$ evolution [214,215]. Their performance can be improved considerably by introducing catalysts directly onto the semiconductor electrodes as a thin

film or islands, or alternatively photoreducing suitable acceptor relays such as methyl viologen or Co(sepul)$^{3+}$ and subsequently evolving H_2 from reduced relays in the bulk of the electrolyte solution using catalysts. Indeed, several recent studies involving p-InP, p-Si, p-GaAs and p-GaP have amply confirmed both of these possibilities [216–227]. Heller and coworkers in particular have obtained quite impressive solar conversion efficiencies (> 10%) for the photoproduction of H_2 from water using the low-band material p-InP and Pt-group metal catalysts.

Novel photooxidation reactions on n-type semiconductor electrodes assisted by redox catalysts are also currently being explored, and preliminary results reported appear very promising [228–233]. One of the main problems in the effective utilization of otherwise excellent low-band n-type non-oxide semiconductors is the very rapid photocorrosion. Hence, these electrodes need to be protected first with a conducting film such as indium–tin oxide or polypyrrole or an oxide/silicide layer before any redox catalyst can be attempted. Photoelectrochemical generation of Cl_2 at moderate solar conversion efficiencies (3–5%) has been observed on catalytically-modified (RuO_2-incorporated) n-Si with silicide/ITO protective coatings [229,230]. Similarly, light-induced O_2-evolution from water has been observed on RuO_2-deposited n-CdS [232] and n-GaAs electrodes protected with a polypyrrole film [233].

(iii) Heterogeneous photocatalysis with semiconductor particulate systems

In addition to the work on photochemical water cleavage, there is currently extensive research activity in the area of heterogeneous photocatalysis with semiconductor particulate systems. Both "naked" and "catalyst-loaded" semiconductor dispersions are being assayed for various photocatalytic ($\Delta G < 0$) and photosynthetic ($\Delta G < 0$) reactions. Table 6 lists some of these topics, and recent, comprehensive reviews of this area are available [15,16]. Here, we briefly present two areas, that having considerable industrial interest and that of current research activity in our laboratories.

(a) Photocatalytic cleavage of H_2S and thiosulfate synthesis

In addition to H_2O, another hydride of the group, H_2S, is a potentially useful source in the quest for alternatives to fossil fuels. Sulfides are attractive since they occur widely in natural gas fields and are produced in large quantities as an undesirable byproduct in the coal and petroleum industries [234]; in addition oxidation of sulfides to sulfur (eqn. 37) or to polysulfides (eqn. 38) is thermodynamically an easier process
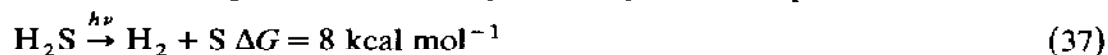
$$H_2S \xrightarrow{h\nu} H_2 + S \quad \Delta G = 8 \text{ kcal mol}^{-1} \tag{37}$$

$$nS^{2-} + S \rightarrow S_n^{2-} \tag{38}$$

TABLE 6

Photocatalytic and photosynthetic reactions on semiconductor particulate systems

Reaction

1. *Studies with "naked" semiconductor dispersions*
   1.1 Photoadsorption and photodesorption of gases
   1.2 Photocatalytic oxidation of CO, H_2, N_2H_4 and NH_3
   1.3 Isotopic exchanges on semiconductor surfaces
   1.4 Photoproduction of H_2O_2 and its decomposition
   1.5 Photooxidation and photoreduction of inorganic substances (CN^-, $S_2O_8^{2-}$, $Cr_2O_7^{2-}$, SO_3^{2-}, $\cdots$)
   1.6 Photodeposition of metals
   1.7 Photoreduction of CO_2 and of N_2
   1.8 Photooxidation of organic materials (alkanes, alkenes, alcohols, aromatics, $\cdots$)
   1.9 Photohydrogenation, photodehydrogenation reactions

2. *Studies with "catalyst-loaded" semiconductor dispersions*
   2.1 "Metallized" semiconductor studies
      2.1.1 Photodecomposition of water
      2.1.2 Photooxidation of halides and cyanides
      2.1.3 Photooxidation of carboneous materials
      2.1.4 Photo-Kolbe reaction
      2.1.5 Photosynthetic production of aminoacids
      2.1.6 Photochemical slurry electrode cells
      2.1.7 Photoassisted water-gas shift reaction
   2.2 *Metal-oxide coated semiconductor studies*
      2.2.1 Photodecomposition of water
   2.2.2 Photodecomposition of H_2S

Aqueous dispersions of CdS, when illuminated by visible light, cleave H_2S with high efficiency. While the reaction proceeds without the intervention of a noble metal catalyst (due to cathodic shifts in V_{fb} upon sulfide adsorption) loading of CdS particles with RuO_2 enhances markedly the efficiency of the process [235,236]. The presence of oxygen has only a small effect on the quantum yield of H_2S cleavage. Addition of ionic surfactants greatly affects the efficiency of "naked" semiconductor dispersions, with a fourfold increase in quantum yield achieved by the addition of sodium lauryl sulfate, at concentrations below the CMC.

Marked improvements in performance are also observed upon addition of SO_3^{2-} in studies with RuO_2-loaded dispersions [236–240]. The intervention of sulfite is rather indirect and involves reaction with S to yield $S_2O_3^{2-}$

$$S + SO_3^{2-} \rightarrow S_2O_3^{2-} \tag{39}$$

The reaction in the presence of sulfite is attractive for two reasons. First, thiosulfate is a more valuable product than sulfur since it is used in

industrial processes such as photography. Secondly, sulfite favorably affects the rate of H_2S photocleavage, and removal of sulfur makes it possible to sustain the reaction over long periods. The overall reaction corresponds to the photogeneration of H_2 and $S_2O_3^{2-}$ via

$$S^{2-} + SO_3^{2-} + 2H_2O \overset{2h\nu}{\rightarrow} S_2O_3^{2-} + H_2 \tag{40}$$
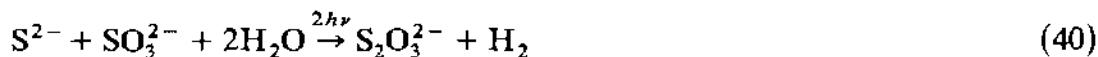
While the above reaction under standard conditions (pH 14, 298 K) stores only 0.11 eV of free energy per absorbed photon, compared with 0.36 eV for the cleavage of H_2S, it has the advantage over the latter process in giving high yields of H_2 without formation of insoluble products.
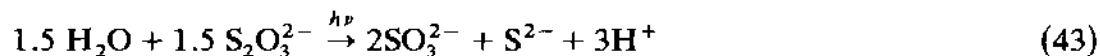
For sustained H_2 production in a cyclic system, it is of interest to couple the process in reaction (40) with one capable of converting $S_3O_3^{2-}$ back to S^{2-} and SO_3^{2-}. We have found that conduction band electrons produced by bandgap excitation of TiO_2 particles efficiently reduce $S_2O_3^{2-}$ to S^- and SO_3^{2-}

$$2e_{cb}^-(TiO_2) + S_2O_3^{2-} \rightarrow S^{2-} + SO_3^{2-} \tag{41}$$

This reaction was confirmed by electrochemical investigation with polycrystalline TiO_2 electrodes [241]. The valence band process in alkaline TiO_2 dispersions involves oxidation of $S_2O_3^{2-}$ to tetrathionate which quantitatively dismutates into SO_3^{2-}, the net reaction being

$$2h^+(TiO_2) + 0.5\ S_2O_3^{2-} + 1.5\ H_2O \rightarrow SO_3^{2-} + 3H^+ \tag{42}$$
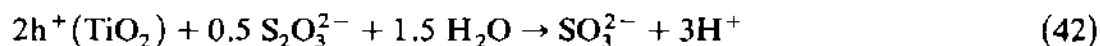
This photoinduced disproportionation of $S_2O_3^{2-}$

$$1.5\ H_2O + 1.5\ S_2O_3^{2-} \overset{h\nu}{\rightarrow} 2SO_3^{2-} + S^{2-} + 3H^+ \tag{43}$$

should be of great interest for systems that photochemically cleave H_2S into H_2 and S.

In the light of these discussions, experiments on TiO_2–CdS mixed semiconductors are of interest [242]. Recently, we observed that addition of TiO_2 to naked CdS decreased the rate of H_2 production, $r(H_2)$ and deposition of Pt on TiO_2 virtually suppressed H_2 evolution from H_2S. By contrast, RuO_2-loaded TiO_2 mixed with CdS exhibits a remarkable increase in $r(H_2)$. In fact, the efficiency of this system is superior to that from direct loading of RuO_2 on to CdS. We interpret the results as due to interparticle electron transfer from the conduction band of CdS to that of TiO_2.

(b) Photodegradation of organic wastes and pollutants

Photocatalytic processes for the non-biological conversion of materials which are common waste products of biomass and the biomass processing industry to a fuel and/or chemicals are also of potential interest. Thus, photocatalytic reaction of glucose, the most common biomass building

block, in the presence of $TiO_2/RuO_2/Pt$ [243] or TiO_2/Pt [244,245] gives H_2 and CO_2. The mechanism of the process probably involves dehydrogenation of the hydroxyl functional groups of the organic compounds, and probably of aldehydes, with the formation of H_2 and carboxylic acids. These last compounds are then available for decarboxylation via a photo-Kolbe reaction resulting in CO_2 evolution and a shorter chain alcohol which can continue to undergo oxidation. The end products are then only H_2 and CO_2.

A large variety of other biomass sources such as proteins and fats, i.e. organic products in general, have also been examined [244]. Their photocatalytic conversion into H_2, CO_2 and other various simple compounds has considerable potential in cleansing stream waists. Another undesirable class of compounds present in the environment are organochlorinated compounds. Until now, little attention has been devoted to heterogeneous photo-assisted catalytic degradation of such compounds [246], but recently some haloaliphatic compounds were investigated [247].

Haloaromatic compounds include several toxic and harmful materials. 4-Chlorophenol degradation through a heterogeneous photoassisted process using TiO_2 suspensions has proved to give a complete mineralization into CO_2 and HCl [248]. The mass balance of chlorine also precludes formation of other chlorine-containing organic or inorganic derivatives. In addition to light and the semiconductor, the presence of O_2 and water was essential for the process to proceed at a significant rate. The mechanism probably proceeds through an oxygen-containing radical attack and concomitant Cl reduction to Cl^- by conduction band electrons. Further oxidation of the dihydroxybenzene ring breakdown components leads to the final simple products. It is noteworthy that a solar experiment, performed on a sunny day in Torino, Italy, (70–75 mW cm^{-2}) showed complete degradation of 4-chlorophenol within a few hours.

It is worthwhile remembering that, since the extent of toxicity is related to the chlorine content, even partial dechlorination would prove useful in the degradation of environmentally-dangerous chlorinated pollutants. Finally, since photoprocesses involving inorganic pollutants such as SO_3^{2-}, CN^- or heavy metal ions have been already reported and photodegradation of surfactants [249] recently achieved, the prospects for potential application of these processes are indeed bright.

G. ASPECTS OF PHOTOCHEMISTRY AND PHOTOELECTROCHEMISTRY IN COLLOIDAL SEMICONDUCTOR SYSTEMS

(i) Light energy harvesting and charge storage

We started our work on colloidal semiconductors about six years ago while scrutinizing highly-dispersed redox catalysts suitable for the photo-

decomposition of water into hydrogen and oxygen [188]. Titanium dioxide attracted us since it was known from the work of Krasnovsky [250] and Honda [251] that this material could act as a photocatalyst for the oxidation of water to oxygen. Furthermore, TiO$_2$ powders had been reported to split water under UV-light illumination [165,166,168] albeit with small efficiency. The idea of using colloidal semiconductors appeared promising for two reasons: intuitively, one would expect an enhanced catalytic activity for small particles having a large ratio of surface-to-bulk atoms. Furthermore, if success was achieved in producing transparent semiconductor sols, the application of laser photolysis technique could be envisaged to monitor the extremely fast interfacial charge-transfer events occurring in these systems. This would open up a convenient way to analyze and rapidly optimize the catalytic events leading to water decomposition in these systems. Nozik [252], in his famous paper on photochemical diodes, had already discussed the general idea of using colloidal semiconductors in energy conversion devices. However, no specific experiments were reported.

The first transparent TiO$_2$ sol was produced by hydrolyzing titanium tetraisopropoxide in acidic solution [188]. Subsequently, an alternative route was developed which used TiCl$_4$ as the starting material [253]. Controlled hydrolysis in ice-cold water produces particles with an average diameter of 100 Å as determined by electron microscopy and light-scattering techniques. These particles consist of a mixture of anatase and amorphous TiO$_2$ and their point of zero zeta potential was determined as 4.7 [253].

Due to the small particle size there is only little light scattering in the visible. Below 390 nm the absorption rises steeply towards the UV which confirms the 3.2 eV ($\lambda = 388$ nm) band gap of anatase. It is convenient to express the extinction of light by a semiconductor as the reciprocal absorption length α (cm^{-1}) which can be calculated from the absorbance of the solution, A, by the expression [254]

$$\alpha = 1000\,(A/cl)\rho \tag{44}$$

where c is the concentration of TiO$_2$ (in g/l), l is the length of the optical path and ρ is the density of the particles, e.g. for $\lambda = 320$ nm the value of α is 2.6×10^4 cm^{-1}. This implies that light of wavelength 320 nm is extinguished to 90% after traversing 3900 Å or 39 TiO$_2$ particles of 100 Å diameter.

The absorption of light leads to the generation of electron-hole pairs in the colloidal particles which are oriented in a spatially-random fashion along the optical path

$$TiO_2 \xrightarrow{h\nu} TiO_2(e_{cb}^- + h^+) \tag{45}$$

These charge carriers subsequently recombine or diffuse to the surface where they can undergo reaction with suitable scavengers. A simple model developed by us earlier [255] shows that the average diffusion time is given by

$$\tau_d = \left(r_0^2/\pi^2 D \right) \tag{46}$$

where r_0 is the particle radius and D the diffusion coefficient of the respective charge carrier.

More sophisticated models taking into account the presence of a field in the particle have since been derived. Using the linearized Poisson–Boltzmann equation, Albery and Bartlett [256] have derived the potential distribution in a spherical semiconductor particle. They obtained for the difference in the potential at the center ($r = 0$) and at a distance r the relation

$$\Delta\phi = (kT/6e)\left(\frac{r - (r_0 - W)}{L_D} \right)^2 \left(1 + \frac{2(r_0 - W)}{r} \right) \tag{47}$$

where

$$L_D = \left(\epsilon kT/8\pi e^2 \left({}^1 N_d \right) \right)^{1/2}$$

is the Debye length of the semiconductor with a dielectric constant ϵ and a dopant concentration of ${}^1 N_d$ (cm^{-3}), e is the elementary charge, k is the Boltzmann constant and W is the depletion layer width. We discuss here two limiting cases of eqn. (47) which are particularly important for photocatalysis by semiconductor dispersions. First, a situation is considered where the size of the particles is much larger than the depletion layer width ($r_0 \gg W$). Taking into account that under these conditions the relation $r_0 \simeq r$ holds within the depletion layer, eqn. (47) gives

$$\Delta\phi = \left(\frac{kT}{2e} \right)\left(\frac{r - (r_0 - W)}{L_D} \right)^2 \tag{48}$$

and for $r = r_0$

$$\Delta\phi_0 = (kT/2e)(W/L_D)^2 \tag{49}$$

where $\Delta\phi_0$ corresponds to the total potential drop in the semiconductor particle. Note that eqns. (48) and (49) are identical with those obtained for planar electrodes. Apparently, for large particles the spherical geometry does not affect the potential distribution within the semiconductor.

The second case to consider is that of very small (colloidal) semiconductor particles for which the condition $W = r_0$ holds, when eqn. (47) reduces to

$$\Delta\phi = (kT/6e)(r/L_D)^2 \tag{50}$$

and for the maximum potential drop

$$\Delta\phi_0 = (kT/6e)(r_0/L_D)^2 \tag{51}$$

The presence of a field in the particles reduces the transfer time of the minority carrier from the particle interior to the surface, since in this case the Debye length L_D has to be used in eqn. (48) instead of the radius [256]. However, as has been pointed out by Curran and Lamouche [257], the potential drop in the particle has to be at least 50 mV in order for migration to dominate over diffusion. Relatively high dopant levels are required to obtain such $\Delta\phi_0$ values in colloidal semiconductors. For example, to produce a 50 mV potential drop in a colloidal TiO_2 particle with $r_0 = 50$ Å, a concentration of 5×10^{19} cm^{-3} of ionized donor impurities is needed. Intrinsic TiO_2 colloid has certainly a much lower donor concentration and field effects on charge carrier motion in the particles can therefore be neglected.
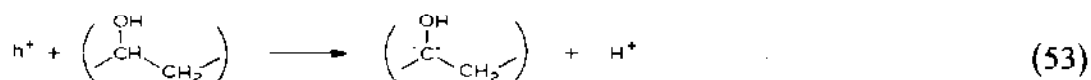
From these considerations it may be seen that τ_d is at most several picoseconds for colloidal semiconductors. For example, in the case of TiO_2 which, due to its heavy effective electron mass, $m_{eff} = 30$ m_e [258], has a relatively small diffusion coefficient, $D_{e^-} = 2 \times 10^{-2}$ cm^2 s^{-1}, a value for τ_d of 2.5 ps may be obtained, using eqn. (46) and a particle radius of 50 Å [259]. This transit time is much faster than the lifetime of an electron hole pair in the TiO_2 particle, which has recently been determined by picosecond laser spectroscopy as 24 ns [260]. Thus, by using highly dispersed semiconductors as light-harvesting units, it is in principle possible to drive photochemical reactions with quantum yields approaching unity.

Whether such high quantum yields can really be achieved depends on the rapid removal of at least one of the types of charge carrier once it reaches the interface. The two processes of importance here are interfacial charge transfer to a solution species or to a catalyst deposited on to the particle and reaction with surface groups of the semiconductor. In aqueous dispersions of oxide semiconductors such as TiO_2, hydroxide ions are present at the surface which can trap positive holes. Note that there are two types of OH^- groups, basic and acidic [261]. The former are attached to one Ti^{4+} ion while the latter bridge two Ti^{4+} sites. Since the electron density is higher on basic OH^- ions, it is expected that these act as the hole traps

$$\tag{52}$$
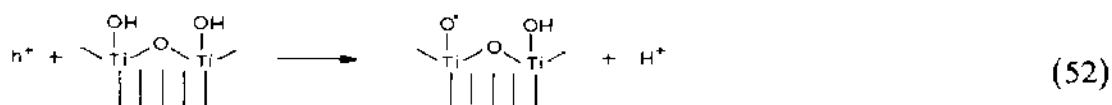
The standard free energy change associated with this reaction has recently been derived from luminescence experiments as -1.4 eV [262]. Thus, basic hydroxide groups at the surface of TiO_2 can be considered as deep traps for valence band holes. Once the positive hole is trapped at such an OH^- site, it can be considered as a surface-bound oxygen radical ($\cdot O^-$). This species has

a surprisingly low cross section for recombination with conduction band electrons ($\sigma \sim 10^{-16}$ cm^2 [263]). As a consequence, a small fraction of 'O$^-$ can escape from recombination with e_{cb}^- and can undergo dimerization at the particle surface to form stable titanium peroxide [190]. This explains why irradiation of TiO$_2$ suspensions produces excess electrons in the particles leading to a downward shift in their isoelectric point [264]. While in pure TiO$_2$ colloids electron accumulation is very limited due to charge recombination, it can be greatly enhanced in the presence of hole scavengers such as polyvinylalcohol (PVA). In the latter case, holes are removed via the reaction [265]

$$h^+ + \left(\begin{array}{c} OH \\ | \\ CH \\ CH_2 \end{array}\right) \longrightarrow \left(\begin{array}{c} OH \\ | \\ C \\ CH_2 \end{array}\right) + H^+ \tag{53}$$

allowing for the electrons to accumulate in the particles. Thus, a strikingly intense, beautiful blue color is formed when colloidal TiO$_2$ particles protected by PVA are subjected to bandgap illumination in the absence of air [265,266]. The spectrum shows a maximum at 780 nm and the extinction coefficient of the electron at this wavelength has recently been determined [266] as 800 M^{-1} cm^{-1}. For a delocalized conduction band electron, the extinction coefficient would be expected to increase with high power of wavelength ($\epsilon \sim \lambda^n$). Such free carrier absorption had indeed been observed for colloidal anatase particles by Nozik et al. [267]. The fact that our electron spectrum exhibits a maximum indicates that at least part of the charge carriers are trapped. From studies of thermally-stimulated currents and luminescence, Ghosh et al. [268] concluded that there are at least eight different traps present in rutile with depth levels ranging from 0.21 to 0.87 eV. These traps have been ascribed to point defects, i.e. interstitial titanium ions and oxygen vacancies. Using EPR analysis, the trapped electrons in acidic TiO$_2$ sols have recently been identified as Ti^{3+} located at the particle surface [269].

The possibility of accumulating charges in a reaction space of minute dimensions is a very important feature of colloidal semiconductor particles. It should be recalled that light energy conversion processes such as the cleavage of water in hydrogen and oxygen or the reduction of carbon dioxide involve without exception multi-electron transfer processes. Hence, there is a need for structural organization which provides the possibility of charge storage. In natural photosynthesis, this function is assumed by the plastoquinone assembly in the thylakoid membrane. The colloidal TiO$_2$ particles investigated here provide an inorganic equivalent for such electron reservoirs. The amount of charge that can be stored in these particles is surprisingly high. Thus, from the absorbance change at 780 nm it can be

estimated that ca. 300 electrons are accumulated in one TiO_2 particle corresponding to a carrier density of 5×10^{20} cm^{-3}. Such high electron concentrations are readily accommodated in this semiconductor which, due to its large effective electron mass, has a high density of empty electronic states (N_c) available in the conduction band

$$N_c = 2\left(2\pi m_{eff} kT/h^2\right)^{3/2} \tag{54}$$

For T 298 K, eqn. (54) gives $N_c = 4 \times 10^{21}$ cm^{-3}, which is 8 times higher than the electron concentration measured, indicating that the blue semiconductor particles are not degenerate.

It might be expected that the storage of 300 electrons in a 50 Å-sized particle would produce a large negative shift in its potential with respect to the surrounding aqueous solution. However, the TiO_2/water interface is distinguished by a large double layer capacity, which is 85 μF cm^{-2} at the point of zero charge and increases to 200–300 μF cm^{-2} in alkaline solution [270]. The negative shift in the potential of the particle during accumulation of 300 electrons is therefore only 25 to 90 mV. This explains why such highly-charged particles can be preserved in anaerobic aqueous environment for at least several weeks without giving rise to significant hydrogen generation. The situation appears to be different with colloidal CdS particles where laser excitation has been reported to lead to huge negative shifts in the particle potential resulting in ejection of negative charge carriers and production of hydrated electrons [271].

(ii) Dynamics of interfacial charge transfer processes

Having dealt in detail with the formation, motion and storage of electrons and holes within ultrafine semiconductor particles, we address now the question of interfacial charge transfer. This is a crucial step in the overall light energy conversion process. It is necessary to remove either the electrons or the holes, or both, quickly from the particles in order to avoid charge recombination and to achieve good efficiencies. A strategy frequently employed is to deposit a catalyst at the particle surface which can act as an electron or hole trap. Alternatively, the electrons or holes may be reacted with an appropriate acceptor molecule in solution. In the latter case, the overall reaction is composed of two steps:

(a) Encounter complex formation of the electron (or hole) acceptor with the semiconductor particle. The rate of this process is diffusion-limited and hence determined by the viscosity of the medium and the radius of the reactants.

(b) Interfacial electron transfer. This electrochemical step involves a Faraday current across the semiconductor/solution interface and is characterized by the rate parameter k_{ct} (units cm s^{-1}). Kinetic treatment of this reaction sequence [164,255] yields for the observed bimolecular rate constant for electron transfer the expression

$$\frac{1}{k_{obs}} = \left(\frac{1}{4\pi R^2}\right)\left(\frac{1}{k_{ct}} + \frac{R}{D}\right) \tag{55}$$

where R is the sum of the radii of the semiconductor particle and electron (or hole) acceptor and D is the sum of their respective diffusion coefficients.

Equation (55) establishes an important link between k_{obs}, the familiar rate constant for a second-order reaction and the electrochemical rate parameter k_{ct}. The structure of this equation suggests two limiting cases:

(a) Heterogeneous charge transfer is rate-determining and much slower than diffusion ($k_{ct} \ll D/R$). In this case eqn. (55) reduces to

$$k_{obs} = 4\pi R^2 k_{et} \tag{56}$$

(b) Heterogeneous charge transfer is faster than diffusion, which controls the overall reaction rate ($k_{et} \ll D/R$). In this case the well known Smoluchowski expression is obtained from eqn. (55)

$$k_{obs} = 4\pi DR \tag{57}$$

Finally, note that the influence of diffusion can be eliminated by adsorption or chemical fixation of the acceptor at the semiconductor particle surface. Here, the simple relation

$$k_{ct} = \delta/\tau_{ct} \tag{58}$$

holds where τ_{ct} is the average time required for the charge carrier to tunnel across the interface and δ is the reaction layer thickness.
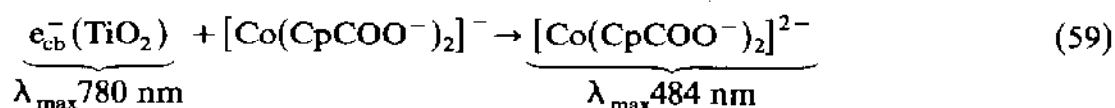
Recently, laser photolysis has been introduced [188,265] as a potent technique for studying the dynamics of charge-transfer reactions at the colloidal semiconductor/solution interface. The transparent nature of these sols renders the application of time-resolved absorption spectroscopy feasible and thus allows for a direct determination of the rate constants for these interfacial redox reactions. We now use the reduction of cobalticinium dicarboxylate by conduction band electrons of colloidal TiO$_2$ as an example to illustrate this procedure. [Co(CpCOO$^-$)$_2$] has shown great promise as a relay compound for hydrogen generation in illuminated chloroplast suspen-

sions [272] or in regenerative photoelectrochemical cells based on p-InP
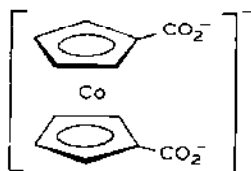
electrodes [222]. Advantages of this mediator are its high chemical stability and relatively weak visible light absorption in both the oxidized and reduced forms. In neutral or alkaline water, reversible one-electron reduction occurs [266,273] at -0.63 V (NHE) rendering thermodynamically feasible the reduction of water to H_2 or of CO_2 to formate.

The kinetics of colbalticinium reduction were recorded by following the decay of the electron absorption at 780 nm and the growth of colbaltocene at 484 nm

$$\underbrace{e_{cb}^-(TiO_2)}_{\lambda_{max}780 \text{ nm}} + [Co(CpCOO^-)_2]^- \rightarrow \underbrace{[Co(CpCOO^-)_2]^{2-}}_{\lambda_{max}484 \text{ nm}} \tag{59}$$

As expected, the rate law was found to be pseudo-first order with respect to cobalticinium dicarboxylate concentration and a second order rate constant of 4×10^4 M^{-1} s^{-1} was evaluated from the kinetic analysis. This is far below the limit imposed by diffusion which for TiO_2 particles with 50 Å radius is calculated as 5×10^{10} M^{-1} s^{-1}. Therefore, the reaction is controlled by the heterogeneous electron transfer at the particle surface and we can apply eqn. (56) to calculate k_{ct}. The value derived is $k_{ct} = 2 \times 10^{-5}$ cm s^{-1} indicating a relatively slow rate for the interfacial redox reaction.

It was discovered during these [266] and other previous investigations [264,265,267,268,274–277] that the rate of charge transfer from oxide semiconductor particles to solution species is strongly affected by the solution pH. This effect was studied particularly thoroughly for colloidal TiO_2 and viologen-type acceptors [264,265,275–277] of the general structure
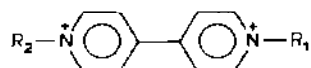
where $E°$(NHE)

$R_1 = R_2 = CH_3$:   methylviologen (MV^{2+}) -0.44 V

$R_1 = R_2 = (CH_2)_3–SO_3^-$:   propylviologen sulfonate (PVS) -0.38 V

$R_1 = CH_3$; $R_2 = (CH_2)_{13}–CH_3$: C_{14} MV^{2+} -0.44 V

and the dimeric viologen [253]

(DV^{4+})
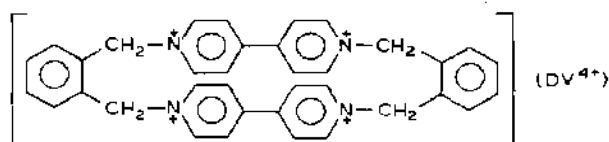
The k_{obs} values for MV^{2+} reduction were determined by monitoring the growth of the 602 nm absorption of the viologen cation radicals after excitation of the TiO_2 colloid [253b,265]. The log k_{obs} versus pH plot is linear in this domain. A striking 10^5 fold increase in the rate constant was obtained when the solution pH was changed from 4 to 10, the slope of the straight line being 0.74. However, the curve bends sharply at higher alkalinity attaining a limit of 5×10^{10} M^{-1} s^{-1}.

These observations can be rationalized in terms of a shift in the position of the conduction band of the colloidal particle with pH. For oxides in contact with aqueous electrolyte H^+ and OH^- are potential-determining ions. (Potential-determining ions play the same role in oxides as do electrons in metal electrodes; changing their concentration changes the potential difference between the particle and the electrolyte.) A simple thermodynamic consideration [278] shows that this potential difference is given by

$$\left(\phi_s^{ox} - \phi^{sol} \right) = \left(\mu_{H^+}^* \right)^{ox} - \left(\mu_{H^+}^* \right)^{sol} + \frac{RT}{F} \ln \frac{\left(a_{H^+} \right)^{sol}}{\left(a_{H^+} \right)^{ox}} \tag{60}$$

where ϕ_s^{ox} and ϕ^{sol} are the potentials at the oxide surface in the plane of adsorption of the potential-determining ions and in solution, respectively, while μ^* designates the standard potential. In the case where $\ln(a_{H^+})^{ox}$ is independent of the particle potential, eqn. (60) simplifies at 25°C to

$$\left(\phi_s^{ox} - \phi^{sol} \right) = \text{const} - 0.059 \text{ pH} \tag{61}$$

Here, the potential difference between particle and solution changes by 59 mV for every pH unit. Criteria for such "Nernstian" behavior have been discussed by Hunter [279]. The surface of oxides is composed of amphoteric sites which can become charged either positively or negatively

$$M-O^- + H^+ \overset{pK_1}{\rightleftharpoons} M-OH \tag{62}$$

$$M-OH + H^+ \overset{pK_2}{\rightleftharpoons} M-OH_2^+ \tag{63}$$

For such a case, the following expression can be derived for the change in the surface potential with pH [279]

$$d\left(\phi_s^{ox} - \phi^{sol} \right)/d\text{pH} = -\left(\frac{2.3 \, kT}{e} \right) - \left(\frac{kT}{2 N_s e^2} \right)\left(\frac{1}{\theta_0} \right)\left(\frac{d\sigma_0}{d\text{pH}} \right) \tag{64}$$

where the first term has a value of -59 mV at room temperature and the second designates the deviation from Nernstian behavior. The surface parameters that influence the magnitude of the deviation are the density of ionizable groups (N_s, cm^{-2}), the change of surface charge (σ_0) with pH and θ_0, which depends on the difference in the equilibrium constants for the surface protonation reactions (62) and (63)

$$\theta_0 = (10^{(pK_1 - pK_2)/2} + 2)^{-1} \tag{65}$$

θ_0 reaches a maximum value of 0.5 in the case where $pK_1 - pK_2$ has a large negative value. This implies that at the point of zero charge the surface concentration of $M-OH_2^+ = MO^-$ groups is very high and equals $N_s/2$. In such a situation Nernstian behavior is expected. For titanium dioxide $\theta_0 = 8.3 \times 10^{-2}$ and $d\sigma_0/dpH = 4 \times 10^{-6}$ C cm^{-2} [280]. In this case eqn. (64) predicts a relatively small deviation (ca. 7 mV) from Nernstian behavior. Flat band potential measurements performed with TiO_2 (rutile) electrodes have shown strictly Nernstian behavior [281,282] which manifests itself by the fact that the conduction band shifts 59 mV negative for every increasing pH unit

$$E_{cb} = +0.1 - 0.059 \times pH \text{ (V, NHE)} \tag{66}$$

The anatase form of TiO_2 has a band gap greater by 200 mV than rutile which results in a more negative position of the conduction band. Using laser photolysis technique [265], we have derived for colloidal anatase particles mixed with amorphous TiO_2 the relation

$$E_{cb} = -0.11 - 0.059 \times pH \tag{67}$$

which shows that these ultrafine particles also exhibit Nernstian behavior. A similar result was obtained by Bard et al. with pure anatase powder [264]. Important for the use of colloidal TiO_2 in water cleavage devices is the fact, expressed by eqn. (67), that the conduction band position is well matched to the hydrogen evolution potential. Thus, over the whole pH domain the reaction

$$e_{cb}^-(TiO_2) + H^+ \rightarrow 0.5 \ H_2 \tag{68}$$

has sufficient driving force to make feasible high rates of hydrogen evolution in the presence of suitable catalysts.

Having derived a relation between conduction band position and pH, we are now able to quantitatively interpret the pH effect on the rate of reduction of acceptors by conduction band electrons. We first define the driving force (overvoltage) for interfacial charge transfer as

$$\eta = E_{cb} - E^\circ(A/A^-) \tag{69}$$

TABLE 7

Heterogeneous rate constants and transfer coefficients for the reduction of acceptors by conduction band electrons of colloidal TiO_2, derived by laser photolysis

Acceptor	k_{ct}^0 (cm s^{-1})	α	Ref.
MV^{2+}	10^{-2} [a]	0.85	253b
MV^{2+}	5×10^{-3} [b]	0.5	255
$C_{14}MV^{2+}$	10^{-3} [a]	0.78	253b
$[Co(C_6H_4COO^-)_2]^-$	2.2×10^{-4} [a]	0.5	266
O_2	10^{-7} [b]	0.57	274
Methyl orange		0.62 [b]	274
$Rh(bipy)_3^{3+}$	0.4 [a]	0.64	253b

[a] TiO_2 colloid prepared via hydrolysis of $TiCl_4$.

[b] TiO_2 colloid prepared via hydrolysis of titanium tetraisopropoxide.

The heterogeneous rate constant for electron transfer from the conduction band of the particle to the acceptor depends on η according to the Tafel relation

$$k_{ct} = k_{ct}^0 \exp(-\alpha \eta F/RT) \tag{70}$$

where k_{ct}^0 is the specific rate at zero driving force and the transfer coefficient. From eqns. (55) and (67) to (70) equation (71) is obtained

$$\left(\frac{1}{k_{obs}}\right) = \left(\frac{1}{4\pi R^2}\right) \left\{ \left(\frac{1}{k_{ct}^0 \exp(\alpha(0.11 + 0.059 \, \text{pH} + E^\circ(A/A^-))F/RT)} \right) + (R/D) \right\} \tag{71}$$

The validity of eqn. (71) was verified by computer analysis of the experimental results. Meanwhile, heterogeneous rate constants and transfer coefficients have been determined for a number of electron acceptors and some representative examples are given in Table 7. As is apparent from these results, k_{ct} varies over almost 7 orders of magnitude, the highest value being obtained for the reduction of the rhodium complex $Rh(bipy)_3^{3+}$ and the lowest one for that of O_2. Oxygen reduction is kinetically slow on most electrode materials and hence it is not surprising to find a relatively small value for the electron transfer rate constant.

For further interpretation of the results in Table 7, it is profitable, at this time to introduce some elementary notions of electron transfer theory. According to current concepts [283], τ_{ct} in eqn. (58) can be expressed as the product of two terms

$$\tau_{ct}^{-1} = (2\pi/\bar{h}) |V(d)|^2 \times (FC) \tag{72}$$

the electron exchange matrix element $V(d)$, and the Franck–Condon weighted density of states FC. $V(d)$ measures the weak interaction energy between the tails of the wave functions for the electron on the donor and on the acceptor and falls exponentially with distance beyond the contact distance d_0

$$|V(d)|^2 = |V(d_0)|^2 \exp(-\beta(d - d_0)) \tag{73}$$

where β is the damping factor. The theoretically estimated [283] or experimentally inferred [284] values of β range from 2.6 to 1.4 Å^{-1}. The value of 2.6 refers to a theoretical calculation where the electron tunnels from one reactant to the other via vacuum [284]. When a medium is present, a value of 1.44 Å^{-1} was roughly estimated [285]. Miller et al. [286] determined from the distance dependence of the electron transfer rates in frozen media a value for β of 1.2 Å^{-1} while Weaver et al. [287,288] obtained 1.3 Å^{-1} for heterogeneous charge transfer from a gold electrode to $Co(NH_3)_5^{3+}$ groups attached to the surface via chemical spacers.

The Franck–Condon overlap integral FC takes account of the strong dependence of electron transfer on reaction exothermicity and the difference between bond length and angles in the reactants and products, expressed by the reorganization energy λ. In the classical limit, and when frequency changes in individual vibrational modes during charge transfer are neglected

$$FC = (4\pi\lambda kT)^{-1/2} \exp\left(-(\Delta G^* + \lambda)^2/4\lambda kT\right) \tag{74}$$

where ΔG^* is the free energy change associated with the electron transfer reaction. Combining eqns. (73) and (74) yields

$$\tau_{ct}^{-1} = (\pi/\lambda kT)^{1/2}(1/\bar{h}) |V(d_0)|^2 \exp(-\beta(d - d_0))$$
$$\times \exp\left(-(\Delta G^* + \lambda)^2/4\lambda kT\right) \tag{75}$$

summarizing the pre-exponential terms with ν_0 gives

$$\tau_{ct}^{-1} = \nu_0 \exp(-\beta(d - d_0)) \exp\left(-(\Delta G^* + \lambda)^2/4\lambda kT\right) \tag{76}$$

The parameter ν_0 reflects the rate constant of electron transfer for optimally exothermic electron transfer between species in contact $(d-d_0)$. At room temperature, ν_0 has a value of ca. $10^{13.3}$ s^{-1} [288]. For interfacial charge transfer over a distance of $d - d_0 = 5$ Å a value for τ_{ct}^{-1} of 5×10^{10} s^{-1} is obtained from eqn. (76) assuming $\beta = 1.2$ Å^{-1} and optimum driving force $(-\Delta G^* = \lambda)$. If $\Delta G^* = 0$ and the reorganization energy $\lambda = 0.5$ eV, τ_{ct}^{-1} equals 3.4×10^8 s^{-1}. Since the reaction layer thickness δ is about $1/\beta \simeq 0.8$ Å, the heterogeneous rate constant at zero driving force $k_{ct}^0 = 2.7$ cm s^{-1} is obtained from eqn. (58).

The k_{ct}^0 values reported in Table 7 are smaller than this limit indicating $\lambda > 0.5$ eV and/or $(d - d_0) > 5$ Å for the acceptors investigated. It should be noted that very high electron transfer rates ($\tau_{ct}^{-1} > 10^8$ s^{-1}) were obtained in cases where the acceptor adheres strongly to the surface of the semiconductor. Examples are the simultaneous two-electron reduction of DV^{4+} in colloidal TiO$_2$ [253] and the reduction of MV^{2+} by conduction band electrons of CdS particles [254,265,289].

The α values reported in Table 7 range from 0.5 to 0.85, where $\alpha = 0.5$ indicates a symmetrical transition state. Caution should be applied in the interpretation of α values exceeding 0.5. The kinetic treatment of interfacial electron transfer reactions presented so far neglects Coulombic effects in the diffusional approach of semiconductor particle and acceptor. Therefore, eqn. (71) is only valid when electrostatic effects are negligible, i.e. the acceptor and/or particle is uncharged or the ionic strength is high. In general, eqn. (71) must be corrected [290] to allow for variation in electrostatic attraction as the pH changes. For example, in the case of the reduction of MV^{2+} by conduction band electrons of colloidal TiO$_2$, Brown and Darwent found empirically [290]

$$\log k_{ct} = \log k_0 + \left(\alpha + \frac{\gamma}{\sqrt{I}}\right)\text{pH} + \frac{\gamma}{\sqrt{I}}\text{PZZP} \tag{77}$$

where $\gamma = 0.04$ is a constant, I is the ionic strength and PZZP the point of zero zeta potential of the particle. Equation (77) shows that for low ionic strength the slope of the d log k_{ct}/dpH plot is increased and does not correspond straightforwardly to the transfer coefficient α. It is furthermore necessary to take the particle size distribution into account when the colloids are polydisperse, since the observed rate constant depends on the particle radius (eqn. (71)). This point has been treated in a very recent paper by Albery et al. [291].

Reactions of valence band holes of colloidal TiO$_2$ with donors such as halides or thiocyanate (SCN$^-$) have also been investigated by pulsed laser techniques [253b,259,292]. The oxidation of these species follows the sequence

$$X^+ \xrightarrow{h^+} X^\cdot \xrightarrow{X^-} X_2^- \tag{78}$$

and results in the formation of X_2^- radical ions which are readily monitored by their characteristic absorption spectra. Kinetic studies show that the hole transfer occurs within the laser pulse indicating that the average time required for charge transfer is less than 10 ns. Apparently, the oxidation involves only X$^-$-species adsorbed to the semiconductor particle. The efficiency of the process follows the sequence Cl$^- <$ Br$^- <$ SCN$^- \simeq$ I$^-$ and

hence is closely related to the redox potential of the $X^-/X^{\cdot}$ couple. The yields of X_2^- radicals decrease sharply with increasing pH, becoming negligibly small at pH > 2.5. This is attributed to competing reaction of h^+ with surface OH groups (eqn. (52)). At higher pH, the latter process is thermodynamically favored over halide oxidation. Apart from this, desorption of X^- from the particle surface occurs as the pH approaches the PZZP. At pH 1 the quantum yields [253b] are in the range of 0.08 (Cl_2^-) to 0.8 (I_2^-). Essentially, similar results have been reported by Henglein [292] although lower quantum yields were obtained. The yields of Cl_2^- and Br_2^- are greatly improved when RuO_2 is deposited on to the TiO_2 particles. Presumably, the RuO_2 plays the role of a hole-transfer catalyst which increases the rate of charge transfer from the valence band of the semiconductor to the halide ion adsorbed on the surface. RuO_2 is commercially employed as an electrocatalyst for chlorine generation from chloride solutions [293]. Enhancement of hole-transfer reactions by RuO_2 has been observed also with semiconductors other than TiO_2 such as CdS [200,265] and WO_3 [294].

An interesting experiment with Na_2CO_3-containing solutions of colloidal TiO_2 has recently been described by Chandrasekaran and Thomas [295]. Oxidation of carbonate by valence band holes and formation of CO_3^- radicals was analyzed by laser photolysis monitoring its characteristic absorption at 600 nm. Under steady-state UV-light illumination formaldehyde is produced and this was attributed to the reaction sequence [295]

$$^{\cdot}CO_3^- + h^+ \rightarrow CO_3 \rightarrow CO + O_2 \tag{79}$$

$$CO + 2e^- + 2H^+ \rightarrow H_2CO \tag{80}$$

Some interesting and more detailed information on the behavior of valence band holes in colloidal TiO_2 has recently become available. The absorption spectrum of h^+ trapped at a surface hydroxyl group has been reported [296] and has a maximum at ~ 470 nm. The relative rate of the trapping reaction (eqn. (52)) with respect to electron-hole recombination has also been derived [297]. Finally, application of picosecond time-resolved laser photolysis opened up a way to monitor directly the dynamics of the charge recombination and trapping processes [260].

(iii) Photoluminescence of colloidal semiconductors

Recently, there have been extensive investigations on the photoluminescence from semiconductor sols [254,265,298–307]. In our laboratory [254], colloidal particles of CdS have been produced by adding H_2S to an aqueous solution of $Cd(NO_3)_2$ (method 1) or by rapid mixing of Na_2S and $Cd(NO_3)_2$ solutions (method 2). These methods yield particles of an average size of 50

and 30 Å, respectively. Each particle is a single crystal with cubic structure [254,302]. The absorption spectrum of type 1 particles exhibits a steep rise below 520 nm. Near the band edge (2.4 eV = 514 nm for CdS) an exponential dependence on photon energy is obtained for the absorption coefficient α [cm^{-1}]

$$\ln \alpha = \beta h\nu/kT \tag{81}$$

The coefficient β has a value of 0.33, which is significantly below that obtained by Dutton [303] for CdS single crystals with hexagonal structure. The whole extinction spectrum of the particles can be calculated from Mie theory which, in the dipolar limit (particle size $\ll$ wavelength of light), gives

$$\alpha = 18\pi X n_0^3 \epsilon_2 / \left(\lambda \left(\epsilon_1 + 2n_0^2 \right)^2 + e_2^2 \right) \tag{82}$$

where X is the volume fraction of the particles in solution, n_0 the refractive index of the solvent and $\epsilon(\lambda)$, $\epsilon_1 + i\epsilon_2$ the complex dielectric constant of the particle. Brus [305] has pointed out that for CdS particles with $r < 50$ Å, $\epsilon(\lambda)$ should become size dependent (quantum size effect) and the absorption edge should shift to the blue. Such an increase in the bandgap with decreasing particle size is predicted from quantum mechanical considerations [304]. The Bohr radius of the first exciton in CdS is given by

$$r_{exc} = \frac{h^2 \epsilon_0 \epsilon}{c^2 \pi m_{eff}} = 24 \text{ Å} \tag{83}$$

(For CdS $\epsilon = 8.9$ and the effective mass of the electron is 0.2 m$_{e^-}$). Hence r_{e^-} is comparable to the dimensions of the type 1 particles but is larger than those of the type 2 sol. As a consequence, the energy of the electron-hole pair is increased leading to a blue shift in the absorption of the CdS at a particle size below 50 Å. At a particle size of 30 Å the bandgap of CdS should be around 3.2 eV [306]. Similar shifts are predicted for other chalcogenides such as ZnS. The luminescence of the semiconductor should also shift to the blue upon decreasing the particle size, and this has been confirmed experimentally [306,307].

While there is by now a wealth of empirical data on luminescence phenomena in colloidal semiconductors, few authors [254,301] have attempted to assign the observed emission. Our analysis [254] was carried out with type 1 CdS sols. In the absence of external activators, red emission was observed which arises from sulfur vacancies (V_S). The latter are common point defects in CdS, and their ready formation

$$CdS \rightarrow CdS_{1-x} + xS + V_S \ (x \ll 1) \tag{84}$$

is the reason for the *n*-type behavior of this semiconductor. Ionization of V_S occurs in two steps

$$V_S \leftrightarrows V_S^+ + e_{cb}^- \tag{85}$$

$$V_S^+ \leftrightarrows V_S^{2+} + e_{cb}^- \tag{86}$$
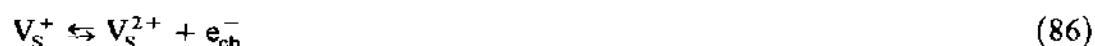
and the Fermi levels associated with these transitions are located at ca. 0.03 [308] and 0.7 eV [309] below the conduction band edge. Red luminescence arises from the reaction of photogenerated holes with ionized sulfur vacancies

$$h^+ + V_S^+ \rightarrow V_S^{2+} + h\nu \ (\lambda = 700 \text{ nm}) \tag{87}$$

and hence is explained by the Lambe–Klick model. The red luminescence is extremely sensitive to the presence of acceptors such as MV^{2+}: 10^{-8} M of MV^{2+} suffices to quench 50% of the emission. Kinetic analysis shows that only one MV^{2+} per CdS aggregate is required to quench the red luminescence, and this effect can be exploited to determine the aggregation number of the particles [254]. The extreme sensitivity of quenching of the luminescence to surface-adsorbed species has also been noted by Brus et al. [298]. PbS and *p*-benzoquinone, along with several others, were found to cause 50% quenching of the luminescence at 10^{-5} M, corresponding to far less than a monolayer surface coverage. SH^--rich CdS colloids undergo a type of photochemical aging if left overnight in room light, during which the initial emission peak at 470 nm red shifts to about 505 nm with a tenfold increase in emission quantum yield. Resonance Raman and electron microscopic studies have been used to confirm this aging process in which about 21 small crystallites (cubic CdS) dissolve and recrystallize onto one large "seed" crystallite. The colloid remains transparent without CdS precipitation as it ages.

At higher concentration, MV^{2+} induces a green emission ($\lambda_{max} = 530$ nm) which was attributed to the formation of cadmium vacancies (V_{Cd}) [254]

$$2(MV^{2+})_{ads} \leftrightarrows 2(MV^+)_{ads} + V_{Cd} + Cd_{aq}^{2+} \tag{88}$$
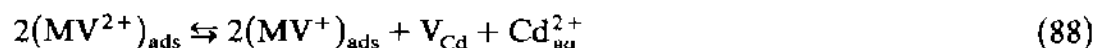
Cadmium vacancies act as acceptors

$$V_{Cd} \leftrightarrows h^+ + V_{Cd}^- \tag{89}$$

and the Fermi level associated with this transition is very close to the valence band [310]. Kuczynski et al. [311] have assigned the green luminescence to viologen–polyphosphate complexes. While Cd vacancies can be formed in CdS particles and do indeed show a green luminescence, the emission observed in the presence of MV^{2+} may also arise from oxidation products of methyl viologen which are produced in MV^{2+}/CdS solutions, presumably under the action of light [312].

(iv) Photosensitized electron injection in colloidal semiconductors

The photosensitization of electron transfer across the semiconductor solution interface plays a vital role in silver halide photography [313] and electro-reprography [314]. Recently, it has also become relevant to information storage and light energy conversion in photoelectrochemical cells [315–319]. In these systems, the phenomenon of photosensitized electron injection is used to effect charge separation with light of less than bandgap energy. Of particular importance for the development of artificial photosynthetic devices is the sensitization of semiconducting oxides such as TiO_2 [320–322], SnO_2 [323] and ZnO [324].

While much pertinent information has been gathered over the years on the overall performance of dye-sensitized semiconductor systems [325], more precise data about the details of the electron injection process are urgently required. The rapid nature of these reactions requires applications of fast kinetic techniques which, in the case of solid semiconductor electrodes or powders, is very difficult. On the other hand, the dynamics of electron injection can readily be investigated with colloidal semiconductors by application of flash photolysis. This is a relatively new field, and only a few studies have appeared so far [326–329]. In the following account, we shall first present experiments that were performed with eosin (EO) and colloidal TiO_2 as a model system, and then discuss application to water cleavage by visible light.

Sensitized electron injection from excited eosin in the conduction band of TiO_2 occurs only under acidic conditions (pH < 7), where the chromophore is strongly adsorbed at the semiconductor surface. The reactive excited state involved in the charge transfer reaction is the singlet and not the triplet state [324]. A similar result has been obtained by Fox [327] for erythrosine sensitization of TiO_2. Due to oxidative quenching, the emission intensity of $EO(S_1)$ is strongly decreased in the presence of colloidal TiO_2. Laser photolysis experiments were performed to identify the products resulting from the quenching reaction. An intense absorption with $\lambda_{max} = 475$ nm was observed arising from the semi-oxidized eosin, EO^+ formed via electron injection from the excited singlet into the TiO_2 conduction band

$$EO(S_1) \rightarrow EO^+ + e_{cb}^-(TiO_2) \tag{90}$$

This mechanism was confirmed by Rossetti and Brus using time-resolved Raman spectroscopy [328]. The quantum yield for charge injection was found to increase with decreasing pH. This effect can be understood by thermodynamic arguments: the driving force for reaction (90) is given by the difference between the redox potential of $EO(S_1)$ and the conduction band position of colloidal TiO_2. For the former, a value of -1.2 V (NHE) is

derived from the ground-state potential and the singlet excitation energy, while the latter is given by eqn. (67). Thus, there is sufficient driving force for reaction (90), even in alkaline solution. Nevertheless, charge injection is only observed at pH 6, i.e. under conditions where eosin is associated with the TiO_2 particles. This is reasonable since close contact of the reactants is required for electron transfer to compete with the other channels of singlet deactivation, i.e. intersystem crossing, as well as radiative and non-radiative deactivation.

The quantum yield for charge injection was also found to decrease at high occupancy of the TiO_2 particles by EO (average number of EO/particle > 30). This effect arises from concentration quenching which occurs under conditions where the distance of adjacent fluorophores approaches their critical radius for dipolar (Förster-type) energy transfer.

We have recently been able to follow the time course of charge injection directly by applying picosecond time-resolved laser flash spectroscopy [330]. The observed rate for EO^+-formation (k_{obs}) is related to the rate constant for charge injection (k_{inj}) via eqn. (91)

$$k_{inj} = k_{obs}\phi(EO^+) \tag{91}$$

where $\phi(EO^+)$ is the quantum yield for EO^+ formation. At pH 3, $k_{obs} = 2.5 \times 10^9$ s^{-1} and $\phi = 0.38$. The rate constant for charge injection is therefore $k_{inj} = 8.5 \times 10^8$ s^{-1}. Practically, the same value was derived earlier from quantum yield analysis [329]. This is a high injection rate which is only a factor of 60 below the limiting value of 5×10^{10} s^{-1} predicted by eqn. (76) for interfacial electron transfer over a distance of 5 Å at optimum driving force ($\Delta G^* = -\lambda$). At pH 3, reaction (57) is thermodynamically downhill by ca. 1 eV. Thus, a relatively high expenditure of free energy is necessary to make the rate of electron injection competitive with other deactivation processes of the excited singlet state. This renders eosin impractical for solar energy conversion devices where sensitization of large bandgap semiconductors is desired. Nevertheless, the eosin/colloidal TiO_2 system lends itself to a study of the salient kinetic features of photosensitized electron injection in semiconductor particulates. Thus, it is possible to obtain information about light-induced charge separation in these systems. The question of how long the photo-injected conduction band electron can survive before it is recaptured by the dye cation radical is a primordial one for energy conversion. Again, laser photolysis investigations with colloidal semiconductor solutions give important clues as to the nature of these charge recombination processes. Similar to intramicellar reactions [321,332], the intraparticle back-electron transfer from the conduction band to the sensitizer cation follows a first-order law if only one EO^+/e_{cb}^- (TiO_2) pair per particle is involved in the process.

A detailed kinetic evaluation [333] which takes into account the statistics

of EO^+ distribution over the particles gives for rate constants of electron recapture and EO^+ desorption the values $k_b = 1.5 \times 10^5$ s^{-1} and $k_d = 3 \times 10^5$ s^{-1}, respectively.

Comparison of the values obtained for k_b and k_d shows that for eosin/TiO_2 electron injection occurs ca. 5000 times faster than charge recombination. This enables light-induced charge separation to be sustained on a colloidal TiO_2 particle for several microseconds, which is sufficient to trap the electron by a noble metal deposit such as Pt. Once trapped on a Pt site, the electron is immediately converted into a hydrogen atom. Therefore, in the presence of noble metal deposits, the fast intraparticle back reaction is suppressed [329]. These experiments offer the possibility of determining the rate of electron trapping and yielding direct information on the nature of the junction (Schottky or Ohmic) between the TiO_2-support and the noble metal deposit.

A chromophore more suitable than eosin to mediate water photolysis is $Ru(bipy)_3^{2+}$. However, sensitization of TiO_2 by this type of transition metal complex is difficult to achieve. Efficient charge injection requires intimate contact between sensitizer and TiO_2 surface. Chromophores such as $Ru(bipy)_3^{2+}$ or surfactant derivatives associate with TiO_2 only above its point of zero zeta potential [334]. In this pH range, the driving force for electron transfer from the excited dye molecule into the conduction band of the semiconductor is too small for efficient sensitization.

Recently, we have performed [335] water cleavage studies with surface derivatized semiconductor particles. During the course of this work, it was discovered that ruthenium tris(2,2'-bipyridyl-4,4'-di-carboxylate), $Ru(bipy(COO^-)_2)_3^{4-}$, 1, in contrast to $Ru(bipy)_3^{2+}$ is a potent sensitizer of TiO_2. In acidic aqueous solution 1 is strongly adsorbed on to the surface of TiO_2. This chemisorption is undoubtedly brought about the strong interaction of the carboxylate groups of the sensitizer with the positively-charged TiO_2 surface. When TiO_2 particles are introduced into aqueous (pH < 5) solution of 1, a bright red color develops on the particles. The reflectance spectrum of the TiO_2 in the visible is identical with the absorption spectrum of 1 while the supernatant spectrum shows simply the disappearance of free 1. The emission with a maximum 640 nm is efficiently quenched by the TiO_2 [336]. This is due to oxidative quenching of the excited chromophore

$$^*Ru(bipy(COO^-)_2)_3^{4-} \rightarrow Ru(bipy(COO^-)_2)_3^{3-} + e_{cb}^-(TiO_2) \qquad (92)$$

The quantum yield for charge injection was determined as 0.6 ± 0.1. Using eqn. (91) a rate constant of $k_{inj} = 3 \times 10^7$ s^{-1} is obtained. The rate for recapture of conduction band electrons by $Ru(bipy(COO^-)_2)_3^{3-}$ was found to be similar to that observed above for the EO^+ recombination with e_{cb}^-.

Occurrence of efficient charge injection from 1 into the conducting band of TiO_2 was confirmed by photoelectrochemical investigations. These employed a polycrystalline anatase electrode [337]. Loading of the electrode with sensitizer was carried out by dipping it for 30 min in a 1.5×10^{-4} M solution of 1 (pH 4) and subsequent rinsing with water. Coloration of the TiO_2 surface by the chromophore is readily visible. Strikingly high photocurrents under visible light excitation were obtained with such electrodes. Monochromatic incident photon-to-current conversion efficiencies as high as 39% were obtained at the wavelength of maximum absorption in the presence of 10^{-3} M hydroquinone as supersensitizer.

Apart from strong adhesion and efficient charge injection, this effect must be attributed to the roughness of the electrode surface. On a smooth surface, 1 absorbs only ca. 1% of 470 nm light at monolayer coverage. However, the surface of the electrode employed here is rough and porous, the roughness factor being around 100. Such an electrode adsorbs a considerably larger amount of sensitizer than a smooth surface. Combined with the fact that the pores act as a light trap inducing multiple reflection, this might lead to a practically total absorption of incident 470 nm light by the chromophore. The coupling of sensitization of TiO_2 by $Ru(bipy(COO^-)_2)_3^{4-}$ to water oxidation using heterogeneous (RuO_2) and homogeneous oxygen evolution catalysts is presently being investigated.

H. CONCLUSIONS

The catalytic conversion of light into chemical energy is a relatively young field which has received a major impetus from the oil crisis in the beginning of the seventies. Given the short time that has elapsed, the progress made has been enormous. In particular, a wealth of knowledge has been acquired in the area of light-induced and thermal electron transfer processes which constitute a crucial step in the overall conversion process. Research in this area continues to advance very rapidly, a recent highlight being the design of chemically-linked donor and acceptor molecules which allows to unravel the intrinsic features of intramolecular electron transfer processes. The exploration of organized molecular assemblies reaction media of minute size to control kinetically the dynamics of photo-initiated redox events is another focal point in the field of artificial photosynthesis.

The discovery of highly active redox catalysts allowed for the coupling of light-induced charge separation to fuel generating steps. Following the initial work on ultrafine Pt and RuO_2 particles as mediators for the reduction and oxidation of water, respectively, this field has traversed a turbulent phase with hundreds of papers being published within a short time. However, this development has now adjusted to a normal pace. The essential factors

controlling the activity of the noble metal particles are established and a significant effort has gone into optimizing these systems, apart perhaps from the oxygen generation catalyst which still needs to be improved.

The advent of colloidal semiconductor particles has rendered feasible the direct observation of light-induced charge carrier generation, their recombination and reaction with catalysts or molecular acceptors. These investigations will continue to thrive and more sophisticated assemblies, such as surface derivatized particles, will soon be scrutinized. Water cleavage by visible light remains the primary target of such studies although other processes, for example the photochemical splitting of hydrogen sulfide, are also of great interest. Much remains to be done, and the task is perhaps one of the most challenging facing scientists. The availability of new sensitizers which are highly active and endurable makes this a particularly promising area of research.

REFERENCES

1 J.S. Connolly (Ed.), Photochem. Conv. Storage Sol. Energy, Proc. III. Int. Conf., Academic Press, New York, 1981.
2 J. Rabani (Ed.), Photochem. Conv. Storage Sol. Energy, Proc. IV. Int. Conf., Weizman Science Press, Jerusalem, 1982.
3 H. Tsubomura (Ed.), Photochem. Conv. Storage Sol. Energy (Book of Abstracts, V. Int. Conf.), Osaka, 1984.
4 A. Harriman and M.A. West (Eds.), Photogeneration of Hydrogen, Academic Press, London, 1982.
5 M. Grätzel (Ed.), Energy Resources Through Photochemistry and Catalysis, Academic Press, New York, 1983.
6 S. Claesson and B. Holmstrom (Eds.), Sol. Energy—Photochemical Processes Available for Energy Conversion (Project Results: NE: 1982: 14), National Swedish Board for Energy Source Development, Stockholm, 1982.
7 J.R. Darwent, P. Douglas, A. Harriman, G. Porter and M.-C. Richoux, Coord. Chem. Rev., 44 (1982) 83.
8 J. Kiwi, K. Kalyanasundaram and M. Grätzel, Struct. Bonding (Berlin), 49 (1982) 39.
9 K.I. Zamanaev and V.N. Parmon, Russ. Chem. Rev., 52 (1983) 817.
10 L.M. Peter, Spec. Period. Reports: Photochemistry, Royal Society of Chemistry, London, 1983, Vol. 13, p. 569.
11 A. Harriman, Specialist Periodical Reports: Photochemistry, Royal Society of Chemistry, London, 1983, Vol. 14, p. 513.
12 K. Kalyanasundaram and M. Grätzel, Photochem. Photobiol., 40 (1984) 807.
13 F. Cardon, W.P. Gomes and W. Dekeyser (Eds.), Photovoltaic and Photoelectrochemical Sol. Energy Conv. (NATO Adv. Study Inst., Ser. B., Vol. 69), Plenum Press, New York, 1981.
14 M. Grätzel, Acc. Chem. Res., 14 (1981) 376.
15 K. Kalyanasundaram in M. Grätzel (Ed.), Energy Resources Through Photochemistry and Catalysis, Academic Press, New York, 1983, chap. 7, pp. 217–260.
16 K. Kalyanasundaram and M. Grätzel in V.R. Vanselow and R. Howe (Eds.), Chemistry and Physics of Solid Surfaces, Springer Verlag, Berlin, 1984, pp. 111–139.

17 K. Hashimoto, T. Kawai and T. Sakata, Chem. Lett., (1983) 709.
18 T. Yamase and R. Watanabe, Inorg. Chim. Acta, 77 (1983) 193.
19 O. Johansen, A.W.H. Mau and W.H.F. Sasse, Chem. Phys. Lett., 94 (1983) 107.
20 O. Johansen, A.W.H. Mau and W.H.F. Sasse, Chem. Phys. Lett., 94 (1983) 113.
21 T. Yamase, Inorg. Chim. Acta, 76 (1983) L25.
22 J. Hawecker, J.-M. Lehn and R. Ziessel, Nouv. J. Chim., 7 (1983) 271.
23 P.A. Lay, A.W.H. Mau, W.H.F. Sasse, I.I. Creaser, L.R. Gahan and A.M. Sargeson, Inorg. Chem., 22 (1983) 2347.
24 I.S. Shehegoleva and S. Ya. Kuchmii, High Energy Chem., USSR, 17 (1983) 81.
25 M.I. Nenadovic, O.I. Micic, T. Rajh and D. Savic, J. Photochem., 21 (1983) 35.
26 A. Launikonis, J.W. Loder, A.W.H. Mau, W.H.F. Sasse, L.-A. Summers and D. Wells, Aust. J. Chem., 35 (1982) 1341.
27 J.R. Darwent, J. Chem. Soc. Chem. Commun., (1982) 798.
28 V. Houlding, T. Geiger, U. Kölle and M. Grätzel, J. Chem. Soc. Chem. Commun., (1982) 681.
29 C.V. Krishnan, C. Creutz, D. Mahajan, H.A. Schwartz and N. Sutin, Isr. J. Chem., 22 (1982) 98.
30 P.C. Lee, M.S. Matheson and D. Meisel, Isr. J. Chem., 22 (1982) 133.
31 A. Launikonis, J.W. Loder, A.W.H. Mau, W.H.F. Sasse and D. Wells, Irs. J. Chem., 22 (1982) 158.
32 T. Koiso, M. Okuyama, T. Sakata and T. Kawai, Bull. Chem. Soc. Jpn., 55 (1982) 2659.
33 C. Creutz, A.D. Keller, N. Sutin and A.P. Zipp, J. Am. Chem. Soc., 104 (1982) 3618.
34 B.S. Brunschwig and N. Sutin, Chem. Phys. Lett., 77 (1981) 63.
35 M. Maestri and D. Sandrini, Nouv. J. Chim., 5 (1981) 637.
36 A. Harriman and A. Mills, J. Chem. Soc. Faraday Trans. 1, 77 (1981) 2111.
37 A. Harriman, G. Porter and M.-C. Richoux, J. Chem. Soc. Faraday Trans. 2, 77 (1981) 833.
38 A. Harriman and M.-C. Richoux, J. Photochem., 15 (1981) 335.
39 A. Harriman, G. Porter and M.-C. Richoux, J. Chem. Soc. Faraday Trans. 2, 77 (1981) 1939.
40 N.Z. Muradov, Yu. V. Bazutin, A.G. Benzuglaya, E.N. Izakovich and M.I. Rustamov, React. Kinet. Cat. Lett., 17 (1981) 355.
41 M.S. Chan and J.R. Bolton, Photochem. Photobiol., 34 (1981) 537.
42 A.J. Frank and K.L. Stevenson, J. Chem. Soc. Chem. Commun., (1981) 593.
43 S.F. Chan, M. Chou, C. Creutz, T. Matsubara and N. Sutin, J. Am. Chem. Soc., 103 (1981) 369.
44 C.V. Krishnan and N. Sutin, J. Am. Chem. Soc., 103 (1981) 2141.
45 A. Harriman and M.-C. Richoux, J. Chem. Soc. Faraday Trans. 2, 76 (1980) 1618.
46 R.J. Crutchley and A.B.P. Lever, J. Am. Chem. Soc., 102 (1980) 7128.
47 G. Giro, G. Casalbore and P.G. DiMarco, Chem. Phys. Lett., 71 (1980) 476.
48 R. Battaglia, R. Henning and H. Kirsch, Z. Naturforsch., Teil B, 36 (1981) 396.
49 R. Henning, W. Schlamann and H. Kirsch, Angew. Chem., Int. Ed. Engl., 19 (1980) 645.
50 R. Ballardini, A. Juris, G. Varani and V. Balzani, Nouv. J. Chim., 4 (1980) 563.
51 T. Tanno, D. Wöhrle, M. Kaneko and A. Yamada, Ber. Bunsenges. Phys. Chem., 84 (1980) 1032.
52 G. McLendon and D.S. Miller, J. Chem. Soc. Chem. Commun., (1980) 533.
53 K. Kalyanasundaram and M. Grätzel, Helv. Chim. Acta, 63 (1980) 478.
54 T.J. Meyer (Ed.), Progr. Inorg. Chem., Vol. 30, Wiley, New York, 1983.
55 D.B. Rorabacher and J.F. Endicott (Eds.), Mechanistic Aspects of Inorganic Reactions, (ACS Symposium Series 198), American Chemical Society, Washington, 1982.

56 T.J. Meyer, ACS Symposium Series 211 (Inorg. Chem. 21st Century), (1983), p. 157.

57 V. Balzani and F. Scandola, in J.S. Connolly (Ed.), Photochem. Conv. Storage Sol. Energy, (Proc. III Int. Conf.), Academic Press, New York, 1981, ch. 1, p. 1.

58 V. Balzani, F. Bolletta, F. Scandola and R. Ballardini, Pure Appl. Chem., 51 (1979) 299.

59 N. Sutin and C. Creutz, Pure Appl. Chem., 52 (1980) 2717.

60 F. Scandola and V. Balzani, J. Chem. Educ., 60 (1983) 814.

61 N. Sutin and C. Creutz, J. Chem. Educ., 60 (1983) 814.

62 J.A. Mercer-Smith and D. Mauzerall, Photochem. Photobiol., 34 (1981) 407.

63 P. Maillard, S. Gaspard, P. Krause and C. Giannotti, J. Organomet. Chem., 212 (1981) 185.

64 J.H. Fuhrhop, W. Krüger and H.H. David, Justus Liebigs Ann. Chem., (1983) 204.

65 J.M. Shellnutt, J. Am. Chem. Soc., 105 (1983) 7179.

66 K. Kalyanasundaram, J. Chem. Soc. Faraday Trans. 1, 79 (1983) 1365.

67 A. Juris, F. Barigelletti, V. Balzani, P. Besler and A. von Zelewsky, Isr. J. Chem., 22 (1982) 87.

68 F. Barigelletti, A. Juris, V. Balzani, P. Belser and A. von Zelewsky, Inorg. Chem., 22 (1983) 3335.

69 R.J. Crutchley, N. Kress and A.B.P. Lever, J. Am. Chem. Soc., 105 (1983) 1170.

70 N. Kitamara, Y. Kawanishi and S. Tazuke, Chem. Phys. Lett., 97 (1983) 103.

71 S.F. Agnew, M.L. Stone and G.-A. Crosby, Chem. Phys. Lett., 85 (1982) 57.

72 R.J. Crutchley, A.B.P. Lever and A. Poggi, Inorg. Chem., 22 (1983) 2647.

73 R.J. Crutchley and A.B.P. Lever, Inorg. Chem., 21 (1982) 2276.

74 (a) D.P. Rillemma, G. Alen, T.J. Meyer and D. Conrad, Inorg. Chem., 22 (1983) 1617.
   (b) G.H. Allen, R.P. White, D.P. Rillemma and T.J. Meyer, J. Am. Chem. Soc., 106 (1984) 2613.

75 (a) D.M. Klassen, Chem. Phys. Lett., 93 (1982) 383.
   (b) S. Wolfgang, T.C. Strekas, H.D. Gafney, R.A. Krause and K. Krause, Inorg. Chem., 23 (1984) 2650.

76 (a) E.Amouyal, B. Zidler and P. Keller, Nouv. J. Chim., 7 (1983) 725.
   (b) A. Kirsch de Mesmaeker, R. Nasielski-Aniken, D. Maertens, D. Paunels and J. Nasielski, Inorg. Chem., 23 (1984) 377.

77 N. Serpone and M.Z. Hoffmann, J. Chem. Educ., 60 (1983) 853.

78 N. Serpone and M.Z. Hoffmann, Isr. J. Chem., 22 (1982) 117.

79 K. Kalyanasundaram, Nouv. J. Chim., 3 (1979) 511.

80 J.-M. Lehn and J.-P. Sauvage, Nouv. J. Chim., 1 (1977) 449.

81 M. Kirsch, J.-M. Lehn and J.-P. Sauvage, Helv. Chim. Acta, 62 (1979) 1345.

82 G.M. Brown, S.-F. Chan, C. Creutz, H.-A. Schwarz and N. Sutin, J. Am. Chem. Soc., 101 (1979) 7638.

83 Q.G. Mulazzani, S. Emmi, M.Z. Hoffman and M. Venturi, J. Am. Chem. Soc., 103 (1981) 3362.

84 Q.G. Mulazzani, M. Venturi and M.Z. Hoffman, J. Phys. Chem., 86 (1982) 242.

85 M. Chou, C. Creutz, D. Mahajan, N. Sutin and A.P. Zipp, Inorg. Chem., 21 (1982) 3989.

86 H.-A. Schwarz and C. Creutz, Inorg. Chem., 22 (1983) 707.

87 A. Bhattacharya, J. Basu, B. Chatterjee, R.G. Bhattacharya, K. Das and K.K. Rohatgi-Mukerjee, Bull. Chem. Soc. Jpn., 56 (1983) 939.

88 S.S. Saidkanov, A.I. Kokorin, E.N. Savinov, I. Vakov and V.N. Parmon, J. Mol. Catal., 22 (1983) 365.

89 E.N. Savinov, S.S. Saidkanov and V.N. Parmon, Kinet. Catal. (USSR), 24 (1983) 55.

90 J.A. Farrington, H. Ebert and E.J. Land, J. Chem. Soc. Faraday Trans. 1, 74 (1978) 665.

91 P. Keller, A. Moradpour, E. Amouyal and P. Kagan, J. Mol. Catal., 7 (1980) 539.

92 D. Miller and G. McLendon, Inorg. Chem., 20 (1981) 950.

93 P. Keller, A. Moradpour, E. Amouyal and B. Zidler, J. Mol. Catal., 12 (1981) 261.

94 E. Amouyal, B. Zidler and P. Keller, Nouv. J. Chim., 7 (1983) 725.

95 H. Dürr, G. Dörr, K. Zengerle, B. Reiss and A.M. Braun, Chimia, 37 (1983) 245.

96 A. Harriman, G. Porter and A. Wilowska, J. Chem. Soc. Faraday Trans. 2, 80 (1984) 191.

97 M.A. Scandola, F. Scandola, A. Indelli and V. Balzani, Inorg. Chim. Acta, 76 (1983) L67.

98 A.M. Bond, G.A. Lawrence, P.A. Lay and A.M. Sargeson, Inorg. Chem., 22 (1983) 2010.

99 I.I. Creaser, A.M. Sargeson and A.W. Zanella, Inorg. Chem., 22 (1983) 4022.

100 C.-Y. Mok, A.W. Zanella, C. Creutz and N. Sutin, Inorg. Chem., 23 (1984) 2891.

101 P.-A. Brugger, P. Cuendet and M. Grätzel, J. Am. Chem. Soc., 103 (1981) 2923.

102 J.-M. Lehn, J.-P. Sauvage and R. Ziessel, Nouv. J. Chim., 5 (1981) 291.

103 N. Toshima, M. Kuriyama, Y. Yamada and H. Hirai, Chem. Lett., (1981) 793.

104 R.F. Jones and D.J. Cole-Hamilton, J. Chem. Soc. Chem. Commun., (1981) 58.

105 J. Kiwi, E. Borgarello, E. Pelizzetti, M. Visca and M. Grätzel, Angew. Chem. Int. Ed. Engl., 19 (1980) 647.

106 E.R. Buyonova, L.G. Matvienko, A.I. Kokorin, G.L. Elizarova, V.N. Parmon and K.I. Zamaraev, React. Kinet. Catal. Lett., 16 (1981) 309.

107 P. Keller, A. Moradpour and E. Amouyal, J. Chem. Soc. Faraday Trans. 2, 78 (1982) 3331.

108 E. Amouyal, D. Grand, A. Moradpour and P. Keller, Nouv. J. Chim., 6 (1982) 241.

109 D.N. Furlong and W.H.F. Sasse, Aust. J. Chem., 36 (1983) 2163.

110 Y. Okuno, Y. Chiba and O. Yonemitsu, Chem. Lett., (1983) 893.

111 M.D. Delcourt, N. Keghouche and J. Belloni, Nouv. J. Chim., 7 (1983) 131.

112 R. Rafaeloff, Y. Hamvy, J. Binenboym, G. Bamch and L.A. Rajbenbach, J. Mol. Catal., 22 (1983) 219.

113 J. Belloni, M.O. Delcourt and C. Leclerc, Nouv. J. Chim., 6 (1982) 507.

114 G. Nord, B. Pedersen and E. Bjergbakke, J. Am. Chem. Soc., 105 (1983) 1913.

115 B.S. Brunschwig, M.H. Chou, C. Creutz, P. Ghosh and N. Sutin, J. Am. Chem. Soc., 105 (1983) 4832.

116 D. Duonghong, W. Erbs, Shuben Li and M. Grätzel, Chem. Phys. Lett., 95 (1983) 266.

117 N. Serpone and F. Bolletta, Inorg. Chim. Acta, 75 (1983) 189.

118 N. Serpone, G. Ponterini, M.A. Jamieson, F. Bolletta and M. Maestri, Coord. Chem. Rev., 50 (1983) 209.

119 J. Kiwi, M. Grätzel and G. Blondeel, J. Chem. Soc. Dalton Trans., (1983) 2215.

120 G. Blondeel, A. Harriman, G. Porter, D. Arwin and J. Kiwi, J. Phys. Chem., 87 (1983) 2629.

121 V.Ya Shafirovich and V.V. Strelets, Nouv. J. Chim., 6 (1982) 183.

122 M. Kaneko, N. Awaya and A. Yamada, Chem. Lett., (1982) 619.

123 S.W. Gersten, G.J. Samuels and T.J. Meyer, J. Am. Chem. Soc., 104 (1982) 4029.

124 S. Goswami, A.R. Chakravarthy and A. Chakravarthy, J. Chem. Soc. Chem. Commun., (1982) 1288.

125 J.-P. Collin, J.-M. Lehn and R. Ziessel, Nouv. J. Chim., 6 (1982) 405.

126 J. Kiwi, J. Chem. Soc. Faraday Trans. 2, 78 (1982) 339.

127 V.N. Parmon, G.L. Elizarova and T.V. Kim, React. Kinet. Catal. Lett., 21 (1982) 195.

128 G.V. Elizarova, L.G. Matvienko, N.V. Nozhkina, V.N. Parmon and K.I. Zamaraev, React. Kinet. Catal. Lett., 16 (1981) 191.

129 G.L. Elizarova, L.G. Matvienko, N.V. Nozhkina, V.E. Maizlish and V.N. Parmon, React. Kinet. Catal. Lett., 16 (1981) 285.

130 N.K. Khannanov and V. Shafirovich, Dokl. Akad. Nauk, SSSR, 260 (1981) 1418.
131 (a) P.K. Ghosh, B.S. Brunschwig, M. Chan, C. Creutz and N. Sutin, J. Am. Chem. Soc., 106 (1984) 4772.
     (b) C. Minero, E. Lorenzi, E. Pramauro and E. Pelizzetti, Inorg. Chim. Acta, 91 (1984) 301.
132 M. Neumann-Spallart and K. Kalyanasundaram, Z. Naturforsch., Teil B, 36 (1981) 569.
133 A. Harriman, G. Porter and P. Walters, J. Chem. Soc. Faraday Trans. 1, 79 (1983) 1335.
134 A. Harriman and P. Walters, Inorg. Chim. Acta, 83 (1984) 151.
135 A. Harriman, J. Chem. Soc. Dalton Trans., (1984) 141.
136 P.-A. Christensen, A. Harriman, G. Porter and P. Neta, J. Chem. Soc. Faraday Trans. 2, 80 (1984) 1451.
137 H. Nijs, J.J. Fripiat and H. Van Damme, J. Phys. Chem., 87 (1983) 1279.
138 D.H.M.W. Thewissen, N. Eeuwhorst-Reinken, K. Timmer, A.H.A. Tinnemans and A. Mackor, Reel. Trav. Chim. Pays-Bas., 101 (1982) 79.
139 M. Kaneko, N. Awaya and A. Yamada, Chem. Lett., (1982) 619.
140 R. Humphry-Baker, J. Lilie and M. Grätzel, J. Am. Chem. Soc., 104 (1982) 422.
141 K. Chandrasekaran, T.K. Foreman and D.G. Whitten, Nouv. J. Chim., 5 (1981) 275.
142 V.Ya Shafirovich, N.K. Khannanov and A.E. Shilov, J. Inorg. Biochem., 15 (1981) 113.
143 N.K. Khannanov and V.Ya Shafirovich, Dokl. Akad. Nauk, SSSR, 260 (1981) 1418.
144 A. Juris and L. Moggi, Int. J. Sol. Energy, 1 (1983) 273.
145 Y. Okuno, O. Yonemitsu and Y. Chiba, Chem. Lett., (1983) 815.
146 A. Harriman, G. Porter and P. Walters, J. Chem. Soc. Faraday Trans. 2, 77 (1981) 2373.
147 J. Kiwi and M. Grätzel, Chimia, 33 (1979) 289.
148 A. Mills, J. Chem. Soc. Dalton Trans., (1983) 1213.
149 A. Mills, J. Chem. Soc. Chem. Commun., (1984) 1436.
150 C. Creutz, H.A. Schwarz and N. Sutin, J. Am. Chem. Soc., 106 (1984) 3036.
151 A. Harriman and J. Barber in J. Barber (Ed.), Photosynthesis in Relation to Model Systems, Elsevier-North Holland, 1979, ch. 8, p. 244.
152 C. Creutz and N. Sutin, Proc. Natl. Acad. Sci., 72 (1975) 2858.
153 V.Ya Shafirovich, N.K. Khannanov and V. Strelets, Nouv. J. Chim., 4 (1980) 81.
154 A. Harriman, G. Porter and P. Walters, J. Chem. Soc. Faraday Trans. 2, 77 (1981) 2373.
155 J. Desilvestro, D. Duonghong, M. Kleijn and M. Grätzel, Chimia, 39 (1985) 102.
156 K. Kalyanasundaram in M. Schiavello (Ed.), Photoelectrochemistry, Photocatalysis and Photoreactors: Fundamentals and Development, NATO Adv. Study Inst., Series C, 1985, Reidel, Dördrecht, 1985, Vol. 146, pp. 239–269.
157 D.S. Miller, A.J. Bard, G. McLendon and J. Ferguson, J. Am. Chem. Soc., 103 (1981) 5336.
158 M. Spiro and P.L. Freund, J. Chem. Soc. Faraday Trans. 1, 79 (1983) 1649.
159 M. Spiro and P.L. Freund, J. Electroanal. Chem., 144 (1983) 293.
160 P.L. Freund and M. Spiro, J. Chem. Soc. Faraday Trans. 1, 79 (1983) 481.
161 D.S. Miller and G. McLendon, J. Am. Chem. Soc., 103 (1981) 6791.
162 M. Spiro, J. Chem. Soc. Faraday Trans. 1, 75 (1979) 1507.
163 W.J. Albery and P.N. Bartlett, J. Electroanal. Chem., 131 (1982) 137, 145.
164 W.J. Albery and P.N. Bartlett, J. Electroanal. Chem., 139 (1982) 57.
165 A.V. Bulatov and M.L. Khidekel, Izv. Akad. Nauk, SSSR, Sci. Khim., (1976) 1902.
166 G.N. Schrauzer and T.D. Guth, J. Am. Chem. Soc., 99 (1977) 7189.
167 M.S. Wrighton, P.T. Wolczanski and A.B. Ellis, J. Solid State Chem., 22 (1977) 17.
168 H. van Damme and W.K. Hall, J. Am. Chem. Soc., 101 (1979) 437.
169 S. Sato and J.M. White, Chem. Phys. Lett., 72 (1980) 83.

170 T. Kawai and T. Sakata, Chem. Phys. Lett., 72 (1980) 87.

171 K. Domen, S. Naito, M. Soma, T. Onishi and K. Tamaru, J. Chem. Soc. Chem. Commun., (1980) 543.

172 T. Kawai and T. Sakata, Nature, 286 (1980) 474.

173 F.T. Wagner and G.A. Somorjai, Nature, 285 (1980) 559.

174 P.C. Jaeger and A.J. Bard, J. Phys. Chem., 83 (1979) 3146.

175 J.-M. Lehn, J.-P. Sauvage and R. Ziessel, Nouv. J. Chim., 4 (1980) 623.

176 S. Sato and J.M. White, J. Catal., 69 (1981) 128.

177 S. Sato and J.M. White, J. Phys. Chem., 85 (1981) 592.

178 E. Borgarello, J. Kiwi, E. Pelizzetti, M. Visca and M. Grätzel, Nature, 284 (1981) 158; J. Am. Chem. Soc., 103 (1981) 6423.

179 J.-M. Lehn, J.-P. Sauvage and R. Ziessel, Isr. J. Chem., 22 (1982) 168.

180 J.R. Darwent and A. Mills, J. Chem. Soc. Faraday Trans. 2, 78 (1982) 359.

181 T. Sakata, T. Kawai and K. Hashimoto, Chem. Phys. Lett., 88 (1982) 50.

182 E. Borgarello, J. Kiwi, M. Grätzel, E. Pelizzetti and M. Visca, J. Am. Chem. Soc., 104 (1982) 2996.

183 K. Domen, S. Naito, T. Onishi and K. Tamaru, Chem. Phys. Lett., 92 (1982) 433.

184 E. Yesodharan and M. Grätzel, Helv. Chim Acta, 66 (1983) 2145.

185 A. Mills and G. Porter, J. Chem. Soc. Faraday Trans. 1, 78 (1982) 3659.

186 R.S. Magliazzo and A.I. Krasna, Photochem. Photobiol., 38 (1983) 15.

187 J.C. Conesa, J.P. Epinos, A. Fernandez, A.R. Gonazales-Elipe, E.J. Lopez-Melina, G. Munuera, A. Munoz, A. Navio, J. Sanz, J. Soria, Abstract B-40, Proceedings, Fifth International Conference on Photochemical Conversion of Solar Energy, Osaka, Japan, August 26–31, 1984.

188 D. Duonghong, E. Borgarello and M. Grätzel, J. Am. Chem. Soc., 103 (1981) 4685.

189 H. Muraki, T. Saji, M. Fujihira, S. Aoyagi, J. Electroanal. Chem., 169 (1984) 319.

190 E. Yesodharan, S. Yesodharan and M. Grätzel, Sol. Energy Mat., 10 (1984) 287.

191 D. Duonghong and M. Grätzel, J. Chem. Soc. Chem. Commun., (1984) 1547.

192 J. Kiwi and M. Grätzel, J. Phys. Chem., 88 (1984) 1302.

193 B. Gu, J. Kiwi and M. Grätzel, Nouv. J. Chim., 9 (1985) 539.

194 J.R. Harbour, J. Tromp and M.L. Hair, Can. J. Chem., 63 (1985) 204.

195 B.V. King and F. Freund, Phys. Rev. Sect. B, 29 (1984) 5814.

196 S. Sato and K. Yamaguti, Abstract A-40, Proceedings Fifth International 1 Conference on Photochemical Conversion of Solar Energy, Osaka, Japan, August 26–31, 1984.

197 S.A. Naman, S.M. Aliwi and K. Al-Emara, Nouv, J. Chim., 9 (1985) 687.

198 G. Blondeel, A. Harriman, D. Williams, Sol. Energy Mat., 9 (1983) 217.

199 J. Rabani, private communication.

200 N.M. Dimitrijevic, S. Li and M. Grätzel, J. Am. Chem. Soc., 106 (1984) 6565.

201 D. Dünnwald, Ph.D. Thesis, Maximilian University of Munich, West Germany, 1982.

202 D. Meissner, R. Memming, S. Li, S. Yesodharan and M. Grätzel, Ber. Bunsenges. Phys. Chem., 89 (1985) 121.

203 J.R. Harbour, R. Wolkow and M.L. Hair, J. Phys. Chem., 85 (1981) 4026.

204 A.J. Frank and K. Honda, J. Phys. Chem., 86 (1982) 1933.

205 K. Honda and A.J. Frank, J. Phys. Chem., 88 (1984) 5577.

206 (a) M. Kaneko, N. Takabayashi, A. Yamada, Chem. Lett., (1982) 1647.
(b) M. Kaneko, N. Takabayashi, Y. Yamamauchi, A. Yamada, Bull. Chem. Soc. Jpn., 57 (1984) 156.

207 H. Nijs, J.J. Fripiat, H. van Damme, J. Phys. Chem., 87 (1983) 1279.

208 Photodecomposition of Water, Toshiba Corp., Japan, Kokai, Tokky-o Koho Japanese Patent 58, 125 601.

122

209 J. Kiwi and M. Grätzel, Angew. Chem., Int. Ed. Engl., 18 (1979) 624.

210 J. Gonzalez Velasco, Abstract A-57, Proceedings, Fifth International 1 Conference on Photochemical Conversion of Solar Energy, Osaka, Japan, August 26–31, 1984.

211 Catalyst for the Photodecomposition of Water, Sibit Montedison Corp., European Patent 0043 251.

212 H. Nijs, M. Cruz, J. Fripiat, H. Van Damme, J. Chem. Soc. Chem. Commun., (1981) 1026; Nouv. J. Chim., 6 (1982) 551.

213 K.J. Takeuchi, G.J. Samuels, S.W. Gersten, J.A. Gilbert, T.J. Meyer, Inorg. Chem., 22 (1983) 1407.

214 H. Gerischer, N. Müller and D. Haas, J. Electroanal. Chem., 119 (1981) 41.

215 M.P. Dare-Edwards, A. Hamnett and J.B. Goodenough, J. Electroanal. Chem., 119 (1981) 109.

216 F.R. Fan, B. Reichman and A.J. Bard, J. Am. Chem. Soc., 102 (1980) 1488.

217 D.C. Bookbinder, J.A. Bruce, R.N. Dominey, N.S. Lewis and M.S. Wrighton, Proc. Natl. Acad. Sci. USA, 77 (1980) 6280.

218 D.C. Bookbinder, N.S. Lewis, M.G. Bradley, A.B. Bocarsly and M.S. Wrighton, J. Am. Chem. Soc., 102 (1980) 7721.

219 H.D. Abruña and A.J. Bond, J. Am. Chem. Soc., 103 (1981) 6898.

220 R.N. Dominey, N.S. Lewis, J.A. Bruce, D.C. Bookbinder and M.S. Wrighton, J. Am. Chem. Soc., 104 (1982) 467.

221 J.A. Bruce, T. Murahashi and M.S. Wrighton, J. Phys. Chem., 86 (1982) 1552.

222 T. Geiger, R. Nottenberg, M.-L. Pelaprat and M. Grätzel, Helv. Chim. Acta, 65 (1982) 2507.

223 A. Heller, B. Miller and F.A. Thiel, Appl. Phys. Lett., 38 (1982) 282.

224 A. Heller and R.G. Vadimsky, Phys. Rev. Lett., 46 (1981) 1153.

225 E. Aharon-Shalom and A. Heller, J. Electrochem. Soc., 129 (1982) 2866.

226 D.E. Aspnes and A. Heller, J. Phys. Chem., 87 (1982) 4919.

227 A. Heller, E. Aharon-Shalom, W.A. Bonner and B. Miller, J. Am. Chem. Soc., 104 (1982) 6942.

228 P. Salvador, V.M. Fernandez and C. Gutierrez, Sol. Energy Mat., 7 (1982) 323.

229 F.R. Fan, R.G. Keil and A.J. Bard, J. Am. Chem. Soc., 105 (1983) 220.

230 L. Thompson, J. Du Bow and K. Rajeshwar, J. Electrochem. Soc., 129 (1982) 1934.

231 G. Hodes, L. Thompson, J. Du Bow and K. Rajeshwar, J. Am. Chem. Soc., 105 (1983) 324.

232 A.J. Frank and K. Honda, J. Electroanal. Chem., 150 (1983) 673.

233 R. Noufi, J. Electrochem. Soc., 130 (1983) 2126.

234 J.B. Hyne in M.E.D. Raymont (Ed.), Sulfur: New Sources and Uses, ACS Symposium Series 183, Am. Chem. Soc., Washington, DC, 1982; Chem. Tech., (1982) 628.

235 E. Borgarello, K. Kalyanasundaram, M. Grätzel and E. Pelizzetti, Helv. Chim. Acta, 65 (1982) 243.

236 E. Borgarello, M. Grätzel, K. Kalyanasundaram and E. Pelizzetti, Chem. Tech., (1983) 118.

237 E. Borgarello, W. Erbs, M. Grätzel and E. Pelizzetti, Nouv. J. Chim., 7 (1983) 195.

238 D.H.M.W. Thewissen, K. Timmer, M. Eeuwhorst-Reinken, A.H.A. Tinnemans and A. Mackor, Nouv. J. Chim., 7 (1983) 191.

239 N. Bühler, K. Meier and J.-F. Reber, J. Phys. Chem., 88 (1984) 3261.

240 D.H.M.W. Thewissen, E.A. van der Zouwen-Assink, K. Timmer, A.H.A. Tinnemans and A. Mackor, J. Chem. Soc. Chem. Commun., (1984) 941.

241 E. Borgarello, J. Desilvestro, M. Grätzel and E. Pelizzetti, Helv. Chim. Acta, 66 (1983) 1827.

242 N. Serpone, E. Borgarello and M. Grätzel, J. Chem. Soc. Chem. Commun., (1984) 342.

243 T. Kawai and T. Sakata, Nature, 286 (1980) 474.

244 T. Sakata and T. Kawai, Nouv. J. Chim., 5 (1981) 279.

245 M.R. St. John, A.J. Furgala and A.F. Sammells, J. Phys. Chem., 87 (1983) 801.

246 B.G. Olivier, E.G. Cosgove and J.H. Carey, Environ. Sci. Technol., 13 (1979) 1075.

247 A.L. Pruden and D.F. Ollis, Environ. Sci. Technol., 17 (1983) 628; J. Catal., 82 (1983) 418.

248 M. Barbeni, E. Pramauro, E. Pelizzetti, E. Borgarello, M. Grätzel and N. Serpone, Nouv. J. Chim., 8 (1984) 547.

249 H. Hidaka, H. Kubota, M. Grätzel, N. Serpone and E. Pelizzetti, Nouv. J. Chim., 9 (1985) 67.

250 A.A. Krasnovsky and G.P. Brin, Dokl. Akad. Nauk SSSR, 147 (1962) 656.

251 A. Fujishima and K. Honda, Nature, 237 (1972) 37.

252 A.J. Nozik, Appl. Phys. Lett., 30 (1977) 567; Ann. Rev. Phys. Chem., 86 (1978) 241.

253 (a) J. Moser and M. Grätzel, Helv. Chim. Acta, 65 (1982) 1436.
(b) J. Moser and M. Grätzel, J. Am. Chem. Soc., 105 (1983) 6547.

254 J. Ramsden and M. Grätzel, J. Chem. Soc. Faraday Trans. 1, 80 (1984) 919.

255 M. Grätzel and A.J. Frank, J. Phys. Chem., 86 (1982) 2964.

256 W.J. Albery and P.N. Bartlett, J. Electrochem. Soc., 131 (1984) 315.

257 J.S. Curran and D. Lamouche, J. Phys. Chem., 87 (1983) 5405.

258 (a) R.G. Breckenridge and W.R. Hosler, Phys. Rev., 91 (1953) 793.
(b) Y. Yania, Phys. Rev., 130 (1963) 1711.

259 Eqn. (3) is not applicable for semiconductors which have a low effective electron or hole mass since in this case the particle dimension may be commensurate with the size of the charge carrier, c.f. ref. 254.

260 J. Moser, G. Rothenberger, M. Grätzel and N. Serpone, J. Am. Chem. Soc., 107 (1985) 8054.

261 H.P. Boehm, Discuss. Faraday Soc., 52 (1971) 264.

262 Y. Nakato, A. Tsumura and H. Tsubomura, J. Phys. Chem., 87 (1983) 2402.

263 R.H. Wilson, General Electric Technical Information Service, Report No. 79CRD090.

264 M. Ward, J. White and A.J. Bard, J. Am. Chem. Soc., 105 (1983) 27.

265 D. Duonghong, J. Ramsden and M. Grätzel, J. Am. Chem. Soc., 104 (1982) 2977.

266 U. Kölle, J. Moser and M. Grätzel, Inorg. Chem., 24 (1985) 2253.

267 N.M. Dimitrijevic, D. Savic, O. Micic and A.J. Nozik, J. Phys. Chem., 88 (1984) 4278.

268 A.K. Ghosh, F.G. Wakim and R.B. Addis, Phys. Rev., 184 (1969) 979.

269 R. Howe and M. Grätzel, J. Phys. Chem., 89 (1985) 4495.

270 T.W. Healy and L.R. White, Adv. Colloid. Interface Sci., 9 (1978) 303.

271 Z. Alfassi, D. Bahnemann and A. Henglein, J. Phys. Chem., 86 (1982) 4656.

272 P. Cuendet and M. Grätzel, Photochem. Photobiol., 36 (1982) 203.

273 N. El Murr, Transition Met. Chem., 6 (1981) 321.

274 G.T. Brown and J.R. Darwent, J. Chem. Soc. Faraday Trans. 1, 80 (1984) 1631.

275 R. Rossetti and L. Brus, J. Am. Chem. Soc., 104 (1982) 2321.

276 R. Rossetti, S.M. Beck and L. Brus, J. Am. Chem. Soc., 106 (1984) 980.

277 K. Chandrasekaran and J.K. Thomas, J. Chem. Soc. Faraday Trans. 1, 80 (1984) 1163.

278 A. Daghetti, G. Lodi and S. Trasatti, Mat. Chem. Phys., 8 (1983) 1.

279 R.J. Hunter (Ed.), Zeta Potential in Colloidal Science, Academic Press, New York, London, 1981.

280 T.W. Healy, D.E. Yates, L.R. White and D. Chan, J. Electroanal. Chem., 80 (1977) 57.

281 M. Tomkiewicz, J. Electrochem. Soc., 126 (1978) 723.

282 R.N. Noufi, P.A. Kohl, S.N. Frank and A.J. Bard, J. Electrochem. Soc., 126 (1978) 246.
283 R.A. Marcus and P. Siders, J. Phys. Chem., 86 (1982) 622.
284 J.J. Hopfield, Proc. Natl. Acad. Sci. USA, 71 (1974) 3640.
285 I.V. Alexandrov, R.F. Kaimtimov and K.I. Zamaraev, Chem. Phys., 32 (1978) 123.
286 J.R. Miller, J.V. Beitz and R.K. Huddeston, J. Am. Chem. Soc., 106 (1984) 5057.
287 J.T. Hupp and M.J. Weaver, J. Phys. Chem., 88 (1984) 1463.
288 T. Li and M. Weaver, J. Am. Chem. Soc., 106 (1984) 6107; J. Phys. Chem., 87 (1985) 3579.
289 J. Kuczynski and J.K. Thomas, Chem. Phys. Lett., 88 (1982) 445.
290 G.T. Brown and J.R. Darwent, J. Chem. Soc. Chem. Commun., (1985) 93.
291 W.J. Albery, P.N. Bartlett, C.P. Wilde and J.R. Darwent, J. Am. Chem. Soc., 107 (1985) 1854.
292 A. Henglein, Ber. Bunsenges. Phys. Chem., 86 (1982) 241.
293 A.T. Kuhn and C.J. Mortimer, J. Electrochem. Soc., 120 (1973) 231.
294 W. Erbs, J. Desilvestro, E. Borgarello and M. Grätzel, J. Phys. Chem., 88 (1984) 4001.
295 K. Chandrasekaran and J.K. Thomas, Chem. Phys. Lett., 99 (1983) 7.
296 D. Bahnemann, A. Henglein, J. Lilie and L. Spanhel, J. Phys. Chem., 88 (1984) 709.
297 G.T. Brown and J.R. Darwent, J. Phys. Chem., 88 (1984) 4855.
298 R. Rossetti and L. Brus, J. Phys. Chem., 86 (1982) 4470.
299 K. Metcalfe and R.E. Hester, J. Chem. Soc. Chem. Commun., (1983) 133.
300 A. Henglein, Ber. Bunsenges. Phys. Chem., 86 (1982) 301.
301 W.G. Becker and A.J. Bard, J. Phys. Chem., 87 (1983) 4888.
302 R. Rossetti, S. Nakahara and L. Brus, J. Chem. Phys., 79 (1983) 1086.
303 D. Dutton, Phys. Rev., 112 (1958) 785.
304 R. Rossetti, J.L. Ellison, J.M. Gibson and L. Brus, J. Chem. Phys., 80 (1984) 4464.
305 L. Brus, J. Chem. Phys., 79 (1983) 5566.
306 L. Brus, J. Chem. Phys., 80 (1984) 4403.
307 J. Ramsden, S. Webber and M. Grätzel, J. Phys. Chem., 89 (1985) 2740.
308 J.B. Goodenough, private communication.
309 A.A. Vuyesteke and Y.T. Sihronen, Phys. Rev., Sect. C, 113 (1959) 400.
310 I. Uchida, J. Phys. Soc. Jpn., 21 (1966) 645.
311 J.P. Kuczynski, B.H. Milosavijevic, A.G. Lappin and J.K. Thomas, Chem. Phys. Lett., 104 (1984) 149.
312 D.R. Prasad and M.Z. Hoffman, J. Phys. Chem., 88 (1984) 5600.
313 J. Bourdon, J. Phys. Chem., 69 (1965) 705.
314 W.E. Borg and K.H. Hauffe, Current Problems in Electrophotography, de Gruyter, Berlin, 1972.
315 A. Giraudeau, F.R.F. Fan and A.J. Bard, J. Am. Chem. Soc., 102 (1980) 5137 and references therein.
316 P.K. Ghosh and T.G. Spiro, J. Am. Chem. Soc., 102 (1980) 5543.
317 M.P. Dare-Edwards, J.B. Goodenough, A.J Hamnett, K.R. Seddon and R.D. Wright, J. Chem. Soc. Faraday Discuss., 70 (1980) 285.
318 A. Mackor and J. Schoonmann, Recl. Trav. Chim. Pays-Bas, 99 (1980) 71.
319 R. Memming, Surf. Sci., 101 (1980) 551.
320 W.D.K. Clark and N. Sutin, J. Am. Chem. Soc., 99 (1977) 4676.
321 A.H.A. Tinnemans and A. Mackor, Rec. Trav. Chim. Pays-Bas, 100 (1981) 295.
322 A. Hamnett, M.P. Dare-Edwards, R.D. Wright, K.R. Seddon and J.B. Goodenough, J. Phys. Chem., 83 (1979) 3280.
323 M. Gleria and R. Memming, Z. Phys. Chem. N.F., 98 (1975) 303.

324 M. Matsumura, K. Mitsuda, N. Yoshizawa and H. Tsubomura, Bull. Chem. Soc. Jpn., 54 (1981) 692.

325 T. Watanabe, A. Fujishima and K. Honda, in M. Grätzel (Ed.), Energy Resources Through Photochemistry and Catalysis, Academic Press, New York, 1983.

326 J. Kiwi, Chem. Phys. Lett., 102 (1983) 379.

327 P.V. Kamat and M.A. Fox, Chem. Phys. Lett., 102 (1983) 379.

328 R. Rossetti and L. Brus, J. Am. Chem. Soc., 106 (1984) 4336.

329 J. Moser and M. Grätzel, J. Am. Chem. Soc., 106 (1984) 6557.

330 J. Moser, M. Grätzel and N. Serpone, Helv. Chim. Acta, 68 (1985) 1686.

331 M. Maestri, P.P. Infelta and M. Grätzel, J. Chem. Phys., 69 (1978) 1522.

332 M.D. Hatlee, J.J. Kozak, G. Rothenberger, P.P. Infelta and M. Grätzel, J. Phys. Chem., 84 (1980) 1508.

333 G. Rothenberger, private communication.

334 D.N. Furlong and W.H.F. Sasse, Colloids and Surface, 7 (1983) 29; Colloids and Surfaces, 7 (1983) 115.

335 D. Duonghong, N. Serpone and M. Grätzel, Helv. Chim. Acta, 67 (1984) 1012.

336 J. Desilvestro, M. Grätzel, L. Kavan, J. Moser and J. Augustynski, J. Am. Chem. Soc., 107 (1985) 2988.

337 M. Kondelka, A. Monnier, J. Sanchez and J. Augustynski, J. Mol. Catal., 25 (1984) 295.

338 M.M. Taqui Khan, R.C. Bhandwaj and C.M. Jadhav, J. Chem. Soc., Chem., Commun., (1985) 1690.